SPECIAL REPORT 94-12

Structure of Ordinary Ice I_h

Part II: Defects in Ice

Volume 2: Dislocations and Plane Defects

Victor F. Petrenko and Robert W. Whitworth

May 1994

THE UNIVERSITY OF BIRMINGHAM

THAYER SCHOOL OF ENGINEERING 1867

Abstract

This report examines linear and planar defects in ice: dislocations, grain boundaries and stacking faults. The authors review experimental results and theoretical models on the defects' atomic structures and physical properties. In addition, experimental techniques used for direct observation of defects, experimental results and theoretical interpretation of dislocation mobility and the role of dislocations in plastic deformation are considered.

For conversion of SI metric units to U.S./British customary units of measurement consult *Standard Practice for Use of the International System of Units (SI)*, ASTM Standard E380-89a, published by the American Society for Testing and Materials, 1916 Race St., Philadelphia, Pa. 19103.

This report is printed on paper that contains a minimum of 50% recycled material.

Special Report 94-12

US Army Corps of Engineers
Cold Regions Research & Engineering Laboratory

Structure of Ordinary Ice I_h
Part II: Defects in Ice
Volume 2: Dislocations and Plane Defects

Victor F. Petrenko and Robert W. Whitworth

May 1994

Prepared in cooperation with
THAYER SCHOOL OF ENGINEERING
DARTMOUTH COLLEGE
and
SCHOOL OF PHYSICS AND SPACE RESEARCH
THE UNIVERSITY OF BIRMINGHAM

PREFACE

This report was prepared by Dr. Victor F. Petrenko, Professor of Engineering, Thayer School of Engineering, Dartmouth College, Hanover, New Hampshire, and Dr. Robert W. Whitworth, Reader in Crystal Physics, School of Physics and Space Research, The University of Birmingham, Birmingham, U.K. Funding was provided by the U.S. Army Research Office through contract DAAL 03-91-G-0164 and by CRREL.

The authors are most grateful to Dr. George Ashton, Dr. Erland Schulson and the late Dr. Andrew Assur for their help, support and collaboration, without which this report would have had little chance to appear. They also express their special thanks to Dr. Gregory Dash, Dr. Paul Devlin, Dr. John Glen, Dr. Akira Higashi, Dr. Takeo Hondoh, Dr. John Nagle and Dr. Ivan Ryzhkin for their useful remarks and comments on the text. In many cases their suggestions improved the report in content and logic and identified errors that the authors had overlooked. The authors appreciate the help of Linda Dorr, Linda Cuthbert and Oleg Nikolaev in typing and editing the manuscript and in drawing the figures.

CONTENTS

	Page
Preface	ii
Foreword	v
Nomenclature	v
Introduction	1
Dislocations in the ice structure	2
Basal dislocations	2
Nonbasal dislocations	4
Direct observation of dislocations	5
General	5
X-ray topography technique	5
Grown-in dislocations	6
Dislocations associated with plastic deformation	6
Dislocation mobility	8
Experimental observations	8
Peierls model for basal dislocations	9
Proton disorder	10
Role of dislocations in plastic deformation of single crystals	12
Pure crystals	12
Doped crystals and electrical effects	15
Stacking faults	16
Structure of stacking faults in ice	16
Observations of stacking faults	18
Grain boundaries	19
Structure	19
Electrical properties of grain boundaries in doped ice	20
Literature cited	21
Abstract	25

ILLUSTRATIONS

Figure

1. Production of slip in a crystalline material by the glide of a dislocation across the slip plane 1
2. Projection of the structure of ice on the $(1\bar{2}10)$ plane 2
3. Dissociation into two partial dislocations 3
4. Edge dislocation containing a kink on its glide plane and a jog 3
5. Positions of molecules above and below the (0001) glide plane for partial dislocations in ice 4
6. Principle of synchrotron white-beam X-radiation topography 5
7. Topograph projected on the (0001) plane showing concentric dislocation loops in an as-grown crystal of ice 6

Figure Page
8. Topograph projected on the (0001) plane showing dislocations introduced by a compressive stress producing a shear stress 7
9. Sequence of topographs showing edge dislocations propagating on the $(0\bar{1}10)$ and $(\bar{1}010)$ planes from a scratch on the surface of a crystal 7
10. Hexagaonal dislocation loop expanding on the (0001) plane after successive loadings 8
11. Two topographs and a sequence of tracings showing the motion of a pointed dislocation loop 8
12. Dislocation velocities per unit stress in pure ice as functions of inverse temperature 9
13. Computer simulation of glide of a dislocation across a Peierls barrier 10
14. Section in the $(1\bar{1}00)$ plane of a 60° dislocation on a plane of the shuffle set 11
15. Stress–strain curves for tensile deformation of single crystals of ice at –15°C and constant rates 12
16. Operation of a Frank-Read source on the basal plane 13
17. Sequence of topographs projected on the (0001) plane showing operation of a Frank-Read source in ice 14
18. Sequence of topographs projected on the (0001) plane showing dislocation multiplication arising from the fast edge segments 14
19. Test results from pure single crystals of ice and crystals doped with HF 15
20. Projections of structure of ice I_h on a $(1\bar{2}10)$ plane showing stacking faults 17
21. X-ray topograph projected on a (0001) plane of a crystal of pure ice 18
22. Boundary on a $(1\bar{2}11)$ plane between two grains rotated relative to one another . 20
23. Edge dislocation in the boundary produced by shear in the plane of the boundary by small Burger vectors 20

TABLES

Table
1. Activation energies for glide of dislocations in pure ice 9
2. Activation energies for plastic deformation of single crystals of ice 13

FOREWORD

At the present time, thousands and thousands of people around the world deal with ice, snow and permafrost. They are scientists, educators, engineers, navigators, meteorologists and others. While a small fraction of these people contribute to the knowledge base in ice physics, all of them use knowledge from it frequently. Moreover, successful applied research is based upon fundamental science—one more reason for ice specialists to have a textbook on ice physics on their desks.

The first modern ice physics text was Fletcher's book on *The Chemical Physics of Ice* (1970). Fletcher's book is in typical textbook format: it is reasonably brief and easy to understand. He touched on a few of the most important topics, but not all of them.

The most comprehensive book on ice physics to date was published by Hobbs in 1974. Hobbs considered almost all of the basic aspects of ice as understood at that time. Moreover, he described and compared several (sometimes opposing) viewpoints. This fundamental and rather large (837 pages) book is commonly known as the "Ice Bible" by specialists in the field. In 1974 and 1975, two CRREL monographs on ice were produced by John Glen. These were briefly and clearly written and reviewed almost all ice-related subjects. This work was (and in some respects still is) a magnificent introduction to ice.

Finally, in 1981 Maeno wrote a simple, popular book for the express purpose of attracting people's attention to the subject.

During the past 20 years, a significant amount of new experimental and theoretical work has appeared, dramatically changing our views on ice physics. As a result, we are now able to formulate physical laws using more simple and direct methods. We have found some of the physical models used in the past to be completely wrong. The physics of ice is a much better developed subject than it was 20 years ago.

For the above reasons, we feel the time is ripe for a contemporary book on ice physics, incorporating the known and proven with almost 20 years' worth of material not covered by previous works.

We have tried to prepare a "readable" book, and not one that requires the reader to be a uniquely educated person. It is our intent to present the material in such a way that any reader attracted by the title *Ice Physics* will be able to comprehend it. This is quite difficult for a book dedicated, not to a particular field of knowledge, but to a specific material. Indeed, for ice it means we have to consider a wide variety of subjects, including quantum chemistry, solid state physics, the theory of elasticity, ionic conductivity, synchrotron x-ray topography, crystal growth, the physics of surfaces and more.

The primary goal is to produce as simple a book as possible without sacrificing scientific accuracy. Experimental facts, physical ideas and theories will be strongly organized and bound together cohesively. The reader will be introduced to a wide variety of material on a step-by-step basis. Then the picture will be whole.

To accelerate publication, this book will appear first in the form of a series of joint CRREL–Dartmouth reports, later to be published in CRREL's Monograph series, on:

1. The structure of ordinary ice
   Part I: Ideal structure of ice. Ice crystal lattice
   Part II: Defects in ice
      Volume 1: Point defects
      Volume 2: Dislocations and plane defects

2. Electrical properties of ice
   Part I: Conductivity and dielectric permittivity of ice
   Part II: Advanced topics and new physical phenomena
3. Optical properties
4. Electro–optical effects in ice
5. Thermal properties
6. Mechanical properties of ice. Elasticity and anelastic relaxation. Plastic properties. Fracture of ice
7. Electromechanical effects in ice
8. Surface of ice
9. Other forms of ice and their properties
10. Ice in space
11. Ice research laboratories

The reports will be prepared in a sequence convenient to the authors. The present is the fourth in the series.

NOMENCLATURE

This *Nomenclature* section incorporates that of Volume 1, *Point Defects*.

a	lattice constant
$\mathbf{b}$	Burgers vector
b	magnitude of Burgers vector
c	lattice constant
D	diffusion coefficient
D_H	diffusion coefficient of hydrogen in ice
D_i	diffusion coefficient of interstitials
D_s	self-diffusion coefficient
D_{so}	$(va^2)\exp\left(\frac{S_v}{k_B}\right)$
D_v	diffusion coefficient of vacancies
$\vec{D}$	electric displacement vector
e	proton charge
ε	relative dielectric permittivity
$\boldsymbol{\varepsilon}$	strain
E_{aB}	energy of creation of a pair of Bjerrum defects
E_{ai}	energy of creation of an ion pair
E_{as}	activation energy of static conductivity σ_s
$E_{a\infty}$	activation energy of high-frequency conductivity σ_∞
E_f	energy of a defect creation
e_i	defects' electric charge ($i = 1, 2, 3, 4$)
E_{if}	formation energy of interstitials
E_k	kink formation energy
E_{mi}	activation energies of protonic defects' motion ($i = 1, 2, 3, 4$)
ε_o	dielectric permittivity of vacuum
E_s	activation energy of self-diffusion
ε_s	static dielectric permittivity ($\omega << \omega_D$)
$E_{\sigma i}$	activation energy of partial conductivity of i-type defects (i =1, 2, 3, 4)
E_τ	activation energy of Debye relaxation time
E	activation energy
ε_∞	high-frequency ($\omega << \omega_D$) dielectric permittivity
$\dot{\boldsymbol{\varepsilon}}$	strain rate
F	free energy
Φ	$\cong 3.85 k_B T r_{oo}$
f,ν	frequencies
$\mathbf{f}$	fault vector
F_d	free energy of defect formation
F_k	free energy of kink formation
F_m	free energy of kink motion
	force acting on i-type of defects
$\mathbf{g}$	diffraction vector
γ_{ai}	activation volume of formation of protonic defects
γ_{mi}	activation volume of protonic defects' motion
h	separation of the Peierls troughs
η_i	= 1,–1,–1,1 for $i = 1, 2, 3, 4$
j_i	flux density of defects ($i = 1, 2, 3, 4$)
$\vec{J}_{dis}$	displacement current
$\vec{J}_{dr}$	drift current
$\vec{J}, J$	electric current density
k_B	Boltzmann constant
$\mathbf{l}$	unit vector parallel to a dislocation line
μ	mobility
μ_i	mobility of i-type of defects
n	concentration (in m^{-3})
N_d	concentration of dislocations
n_D	D-defect concentration
n_{H_2O}	concentration of water molecules in ice
n_i	concentration of defects ($i = 1, 2, 3, 4$)
n_k	number of kinks per unit length
n_L	L-defect concentration
n_v	concentrations of vacancies
P	pressure
q,e_i	electric charge of carriers
$\dot{Q}$	rate of heat generation
r	distance
r_{oo}	oxygen–oxygen distance in ice lattice (2.76Å)
S	entropy
σ	conductivity
$\boldsymbol{\sigma}$	normal stress
σ_B	Bjerrum defect conductivity—$\sigma_B = \sigma_3 + \sigma_4$
S_c	configurational entropy
S_f	vibrational entropy
σ_i	partial conductivity of i charge carrier
σ_{ion}	ionic conductivity—$\sigma_{ion} = \sigma_1 + \sigma_2$

S_k kink entropy

σ_s static or low-frequency conductivity ($\omega << \omega_D$)

σ_∞ high-frequency conductivity ($\omega >> \omega_D$)

T temperature

τ shear stress

t time

τ_b mean time to reorient a hydrogen bond

τ_D $= \omega_D^{-1}$ Debye relaxation time

τ_L lifetime of charge carriers

U internal energy

U_{im} activation energy of motion of interstitials

U_m activation energy of ionic motion

v_d dislocation velocity

$\vec{v}_d$ drift velocity

V_{if} activation volume of formation of interstitials

V_{im} activation volume of motion of interstitials

v_k kink velocity

V_{mol} molecular volume in ice (3.3×10^{-23} cm^3)

W number of configurations of a system

ω circular frequency

ω_D Debye frequency

$\vec{\Omega}$ configurational vector

x $= n_i/n_{H2O}$

y $= n_D/n_{H2O}$

Structure of Ordinary Ice I_h
Part II: Defects in Ice
Volume 2: Dislocations and Plane Defects

VICTOR F. PETRENKO AND ROBERT W. WHITWORTH

INTRODUCTION

Dislocations are line defects in crystals and are most easily visualized in terms of the slip of one plane of atoms over another by a single lattice spacing, as illustrated in Figure 1. In the intermediate stage shown in this figure, the line BC is the boundary between the slipped region ABC and the remainder of the slip plane. This boundary line is a *dislocation line*, or *dislocation* for short. The presence of the dislocation results in an elastic distortion throughout the whole crystal, but the disruption of the lattice is greatest along the core BC. The lattice vector by which slip has occurred on the plane ABC is known as the *Burgers vector* **b** of the dislocation. Where the dislocation lies parallel to **b** as at B, it is said to have *screw* orientation, and where it is perpendicular to **b** as at C, it has *edge* orientation; in general, a dislocation will have both screw and edge components. An edge dislocation has dangling bonds at its core, as seen in the enlarged region around C shown in Figure 1, and can be thought of alternatively as the line at which an added half-plane of atoms terminates within the crystal. There are no dangling bonds on a screw dislocation, but the lattice is distorted in such a way that a path passing once round the core advances by one Burgers vector.

From the way in which we have introduced them, it is clear that the motion of dislocations on

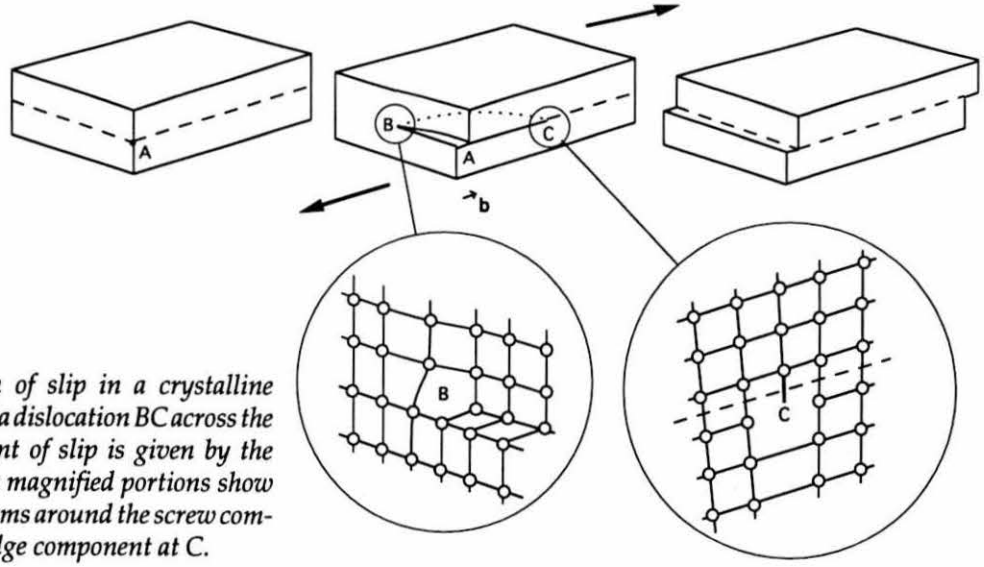

Figure 1. Production of slip in a crystalline material by the glide of a dislocation BC across the slip plane. The amount of slip is given by the Burgers vector **b**. *The magnified portions show the arrangement of atoms around the screw component at B and the edge component at C.*

the slip plane is associated with plastic deformation of the crystal. Such motion of the dislocation is known as *glide*, but it represents only one aspect of the properties of dislocations. Dislocations may be incorporated into a crystal as it is grown, affecting the topology of the whole lattice, but with little effect on plastic deformation. The core of a dislocation may be displaced perpendicular to the glide plane by the adding of atoms to or removing of atoms from the end of the extra half-plane; this is known as *climb*.

The properties of dislocations are described in many books and articles. For a very clear discussion of the basic geometry, we recommend Read (1953), and for a comprehensive discussion including many aspects relevant to ice, Hirth and Lothe (1982). A beautifully illustrated book describing dislocations in ice is that edited by Higashi (1988).

DISLOCATIONS IN THE ICE STRUCTURE

Basal dislocations

It is now well established that crystals of ice deform by slip on the basal plane (0001) (Glen and Perutz 1954), and that macroscopic slip on any other plane is difficult (Higashi 1969, Duval et al. 1983). The Burgers vectors for slip on the basal plane are the three lattice vectors of the form $(a/3)$ $<2\bar{1}\bar{1}0>$, but in macroscopic experiments slip can occur in any direction by a combination of dislocations with these three vectors (Kamb 1961). We will, therefore, consider initially only basal dislocations of this type. Because of the hexagonal symmetry, the simplest dislocations are those that lie parallel or at 60° to the Burgers vector; these are screw and 60° dislocations respectively.

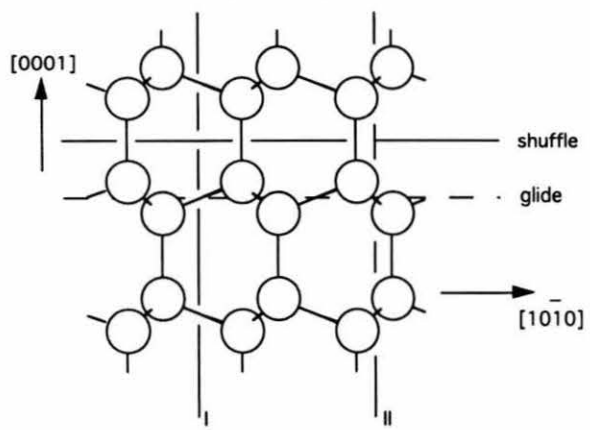

Figure 2. Projection of the structure of ice on the $(1\bar{2}10)$ *plane, showing the basal planes of the shuffle set and of the glide set; I and II are different kinds of* $(10\bar{1}0)$ *planes. Only oxygen atoms are shown.*

Figure 2 shows the ice structure projected on a $(1\bar{2}10)$ plane with the basal plane horizontal. Slip can, in principle, take place between two kinds of planes called the *glide set* and the *shuffle set*. The planes of the shuffle set are more widely spaced and were originally thought to be the natural slip planes, but the planes of the glide set fit over one another in a way that resembles the packing of close-packed metals. On such planes, a dislocation may lower its energy by dissociating into two partial dislocations, separated by a stacking fault (see the *Stacking Faults* section). This dissociation is illustrated in Figure 3a, in which the open and shaded circles represent oxygen atoms on adjacent basal planes of the glide set; the screw dislocation in Figure 3b is shown dissociating into two partial dislocations of Burgers vectors $\mathbf{b}_1$ and $\mathbf{b}_2$ of the type $(a/3)$ $<\bar{1}100>$. Slip by $\mathbf{b}_1$ corresponds to motion of the shaded atoms in Figure 3a from B to C, creating the stacking fault, and slip by the further amount $\mathbf{b}_2$ removes the fault, resulting in a net slip by the full Burgers vector $\mathbf{b} = \mathbf{b}_1 + \mathbf{b}_2$. Both the partial dislocations associated with a screw dislocation have a 30° character. Figure 3c shows the dissociation of a 60° dislocation into an edge and a 30° partial dislocation. The dissociation leads to a reduction in the elastic strain energy of the dislocation, and this reduction is balanced by the energy required to create the stacking fault. From estimates of the stacking fault energy, Fukuda et al. (1987) have estimated that in ice screw dislocations on planes of the glide set would dissociate into partial dislocations separated by about 20 nm.

In many semiconductors with structures related to that of ice, the dissociation of dislocations on the basal plane has been observed directly in the electron microscope, and slip is therefore assumed to occur on planes of the glide set (see George and Rabier 1987). There is no such direct evidence for ice; and, as the bonding is quite different, we cannot presume that the same conclusion applies. However, as we will see, indirect evidence suggests that dislocations do in fact glide on planes of the glide set.

If a straight dislocation lying on its glide plane moves forward by one Burgers vector over part of its length, the step so produced is called a *kink*. An example for an edge dislocation is shown in Figure 4. The most elementary step in the process of glide is for a kink to move along the dislocation by one lattice spacing, as shown by the broken line. Figure 4 also shows a *jog* at which the dislocation makes a step from one glide plane to another. For a dislocation with an edge component, the formation of a

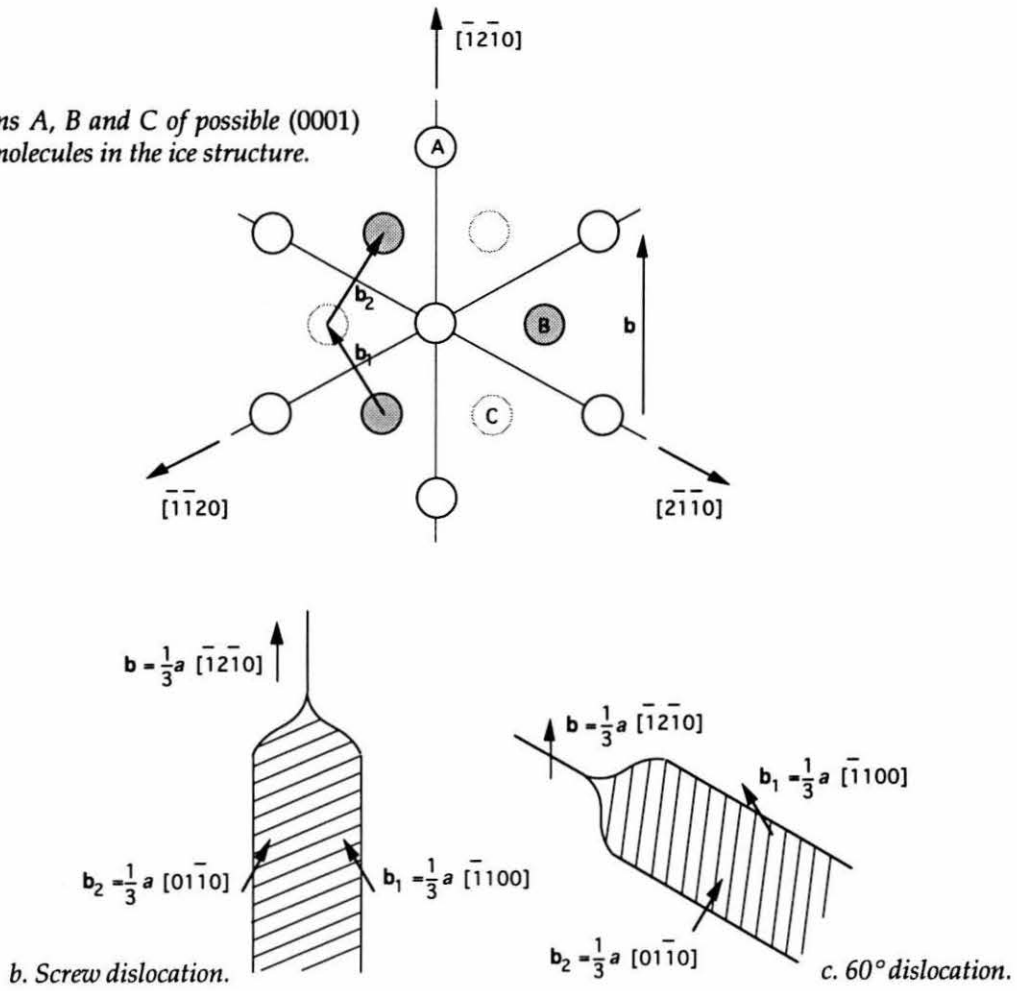

Figure 3. Dissociation into two partial dislocations. Screw and 60° dislocations on planes of the glide set can dissociate into partial dislocations with the Burgers vectors $\mathbf{b}_1$ and $\mathbf{b}_2$ separated by a stacking fault, shown shaded.

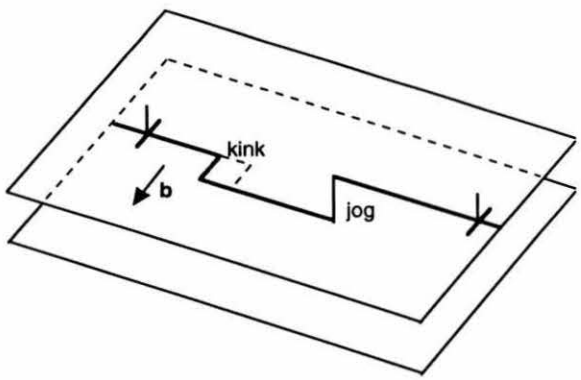

Figure 4. Edge dislocation containing a kink on its glide plane and a jog at which it makes a step from one glide plane to another. The broken line shows an elementary step in the motion of the kink.

jog or its motion along the dislocation requires that atoms be added to or removed from the end of the extra half-plane, and this is what is involved in climb. In this process, the dislocation acts as a source or sink of vacancies or interstitials. In the ice structure, the simplest jog would take the dislocation from a glide to a shuffle plane; a full jog must span two layers of atoms (see Fig. 2).

Kinks and jogs are in general quite different in character. However, a pure screw dislocation has the property that it can, in principle, glide on any plane containing its Burgers vector, and in this case whether a particular step behaves as a kink or a jog depends upon which plane is being considered to be the glide plane.

Figures 5a and b show the arrangement of molecules on the two sides of the basal glide plane at an edge and a 30° partial dislocation in the ice structure (Whitworth 1980). Open circles repre-

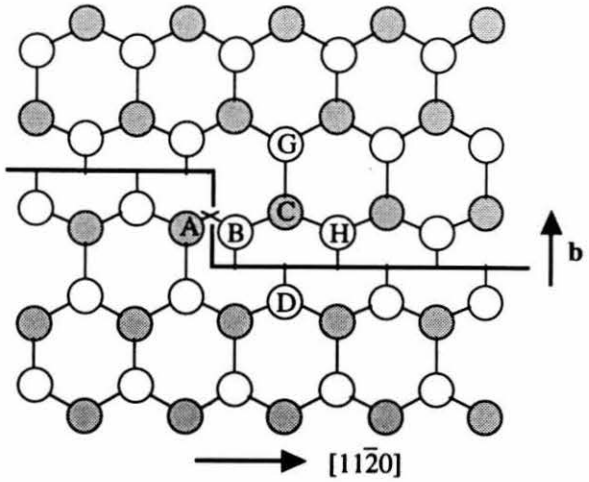

a. Dislocation core for edge dislocations with dangling bonds.

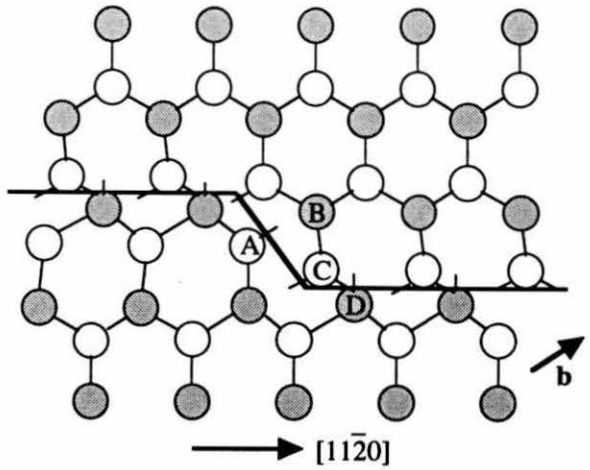

b. Dislocation core with 30° partial dislocations and dangling bonds.

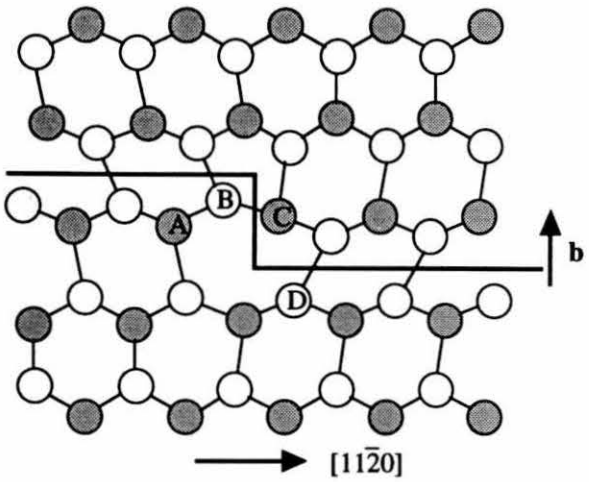

c. Possible way in which the core in Figure 5a can be reconstructed to link up the dangling bonds.

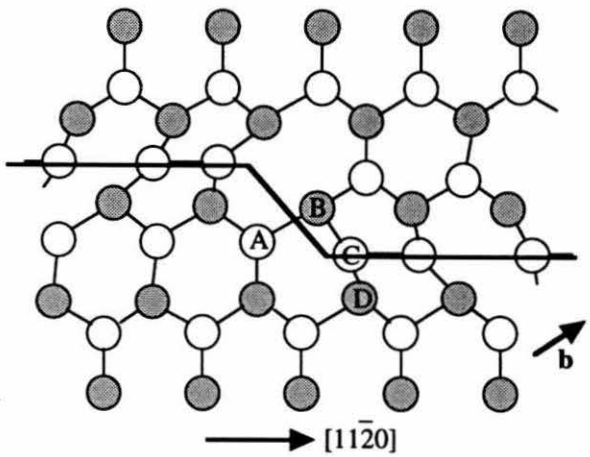

d. Possible way in which the core in Figure 5b can be reconstructed to link up the dangling bonds.

Figure 5. Positions of molecules above and below the (0001) *glide plane for partial dislocations in ice.*

sent molecules above the glide plane and shaded circles represent those below. The extra half-plane is above the glide plane, and the dislocations in both of the diagrams include kinks. There are dangling bonds on the molecules above the glide plane at the edge dislocation, and on both sides of the glide plane for the 30° dislocation. With some changes to bond lengths and bond angles, and with some local elastic distortion, it is possible to link up these dangling bonds, except at the kinks, as shown in Figures 5c and d. This is known as *reconstruction*, which is generally believed to occur in semiconductors. Calculations by Heggie et al. (1992) suggest that it probably happens in ice, too, although there is more than one possibility about how the reconstruction might occur for the 30° dislocation.

Nonbasal dislocations

Dislocations with the basal Burgers vector $(a/3)\langle 2\bar{1}\bar{1}0\rangle$ can in principle glide on the nonbasal planes that include this vector, such as $\{01\bar{1}0\}$ or $\{01\bar{1}1\}$, and in the *Dislocations Associated with Plastic Deformation* section, we will report observations of edge dislocations that glide on such planes. There is again more than one possible type of glide plane, such as the sets of $(10\bar{1}0)$ planes marked I and II in Figure 2, but there is no evidence to show which of these is operative.

In addition we may expect dislocations in which the Burgers vector has a [0001] component. Such dislocations have been observed in ice, usually in the form of loops lying in the (0001) plane. Such loops are called *prismatic* and are formed by the condensation of point defects. There is no evi-

dence that these dislocations can glide or that ice can be deformed plastically by slip in the [0001] direction.

DIRECT OBSERVATION OF DISLOCATIONS

General

Since the earliest experiments of Webb and Hayes (1967), X-ray topography has been extensively used for the study of dislocations in ice. It is undoubtedly the most suitable technique for use with this material, and, of all materials, ice has been the one most fruitfully studied by this method. We will first try to explain why this is so.

For other materials the most powerful technique for observing dislocations is usually the transmission electron microscope. However, in the case of ice, the preparation and handling of suitable thin specimens present enormous difficulties, and, even when prepared, the specimens have a very limited life in the electron beam. Although there have been reports of such experiments (Unwin and Muguruma 1972, Falls et al. 1983), no significant information has been obtained in this way. It is possible to produce etch pits on ice (Higuchi 1958) that can be useful in orienting crystals, but these do not normally correspond to the points of emergence of dislocations. Particular kinds of etch pits and other etch features do appear to be related to dislocations (e.g., Muguruma and Higashi 1963, Sinha 1977), but the information obtained from such experiments is very limited compared with that from other crystals, such as LiF.

In contrast, X-ray topography has been used to reveal dislocations in the interior of crystals that are a few millimeters thick and to observe their motion during annealing and while under stress. This is possible because ice, having a low molecular weight, is sufficiently transparent to X-rays of wavelength less than about 0.9Å, and ice crystals can be grown with a low enough dislocation density, that individual dislocations can be distinguished in such large specimens. A further reason why ice is suitable for dynamic experiments on dislocations is that they can be moved slowly under stress, whereas in many materials dislocations move suddenly by large distances once some critical stress is reached.

X-ray topography technique

The form of X-ray topography that is the simplest and the most easily explained has only become possible with the availability of intense, highly collimated beams of "white" X-radiation from a synchrotron source. If such a beam falls on a single crystal, as shown in Figure 6, it produces Laue diffraction spots, in which there is a one-to-one correspondence between a position on the spot and the position at which the X-rays passed through the crystal. Local misorientations of the lattice within the crystal, such as occur at dislocations, change the diffraction conditions slightly and result in contrast in the Laue spot. Each spot is therefore an image of the crystal in which dislocations are visible, and these images are called topographs. The topographs can be recorded on high-resolution photographic film or plates, and observed in real time at lower resolution with an X-ray sensitive TV camera.

The imaging conditions depend on the diffraction vector $\mathbf{g}$, so that a dislocation of Burgers vector $\mathbf{b}$ will not appear in a topograph for which both $\mathbf{g}\cdot\mathbf{b} = 0$ and $\mathbf{g}\cdot(\mathbf{b}\times\mathbf{l}) = 0$, where $\mathbf{l}$ is a unit vector parallel to the dislocation line. This makes it possible to identify the character of each dislocation.

The resolution depends on the degree of collimation of the incident beam, which can only be satisfactorily achieved with a synchrotron. Without this collimation, we have to use monochromatic radiation, and, with a conventional X-ray source, the beam divergence for a reasonable intensity is then too high for Bragg's law to be satisfied over the whole crystal at once. Provision has then to be made for scanning the crystal across the beam, and the most commonly used arrangement is the Lang (1959) camera, which has been used extensively in all but the most recent work on ice (see review by Higashi 1988). Because of the scan-

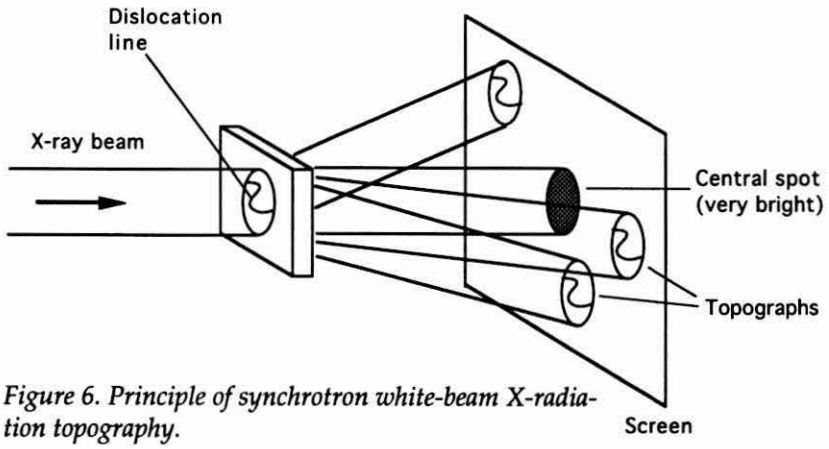

Figure 6. Principle of synchrotron white-beam X-radiation topography.

ning, the exposure time, which is typically a few seconds using a synchrotron, becomes minutes or hours, depending on the power of the X-ray generator.

Observations made by topographic methods fall into three groups—dislocations grown into the crystal, dislocations produced during plastic deformation and dislocations introduced or modified by diffusion processes. The last of these groups was considered by in Volume 1, *Point Defects* (Petrenko and Whitworth [1994] see section on *Molecular Effects*).

Grown-in dislocations

All normally produced crystals (produced without special precautions being taken) or grains within polycrystals contain stable networks of grown-in dislocations, which often form arrays constituting low angle boundaries. In ice almost all such dislocations have the basal Burgers vector, and their concentrations are appreciably lower than those found in metals and other commonly occurring solids. Examples of good quality ice from the Mendenhall Glacier are described by Fukuda and Higashi (1969), but other naturally occurring ice can be much less perfect (Fukuda and Shoji 1988). For the study of individual dislocations by topographic methods, much lower dislocation densities are needed, and much attention has been given in Japan to the growth and examination of such crystals (Higashi et al. 1968, Higashi 1974, Oguro 1988). Single crystals that are several centimeters in diameter and typically 10 cm long are grown in glass tubes that are seeded by growth through a capillary. The latest refinement of this method is that of Ohtomo et al. (1987). Good crystals contain less than 100 dislocations with $(a/3)\langle 2\bar{1}\bar{1}0\rangle$ Burgers vectors per square centimeter, but there are usually also a few circular or spiral loops that have [0001] Burgers vectors and lie on or close to the basal plane (Fig. 7). These loops, which are of prismatic character, have been studied by Oguro and Higashi (1981), and it is now believed that they are formed by the condensation of interstitials (Oguro et al. 1988). Crystals with significant concentrations of impurities are usually much less perfect (Oguro 1988), but the grains within polycrystals grown slowly under carefully controlled conditions can be remarkably good (Liu et al. 1992).

Dislocations with plastic deformation

Many experiments have been described in which dislocations were observed to move and to multiply under an applied stress. Such motion represents an extremely early stage of deformation; once any significant macroscopic strain is produced, the dislocation density becomes too high for topographic observations. In early experiments (e.g., Fukuda and Higashi 1973, Jones and Gilra 1973, Maï 1976, Fukuda et al. 1987, Fukuda and Higashi 1988) much information was lost, because, as was found subsequently, the dislocation structure changed after unloading in the time that was required to obtain the topographs. In more recent work, especially that using synchrotron radiation, it is much easier to identify different kinds of dislocations in the topographs.

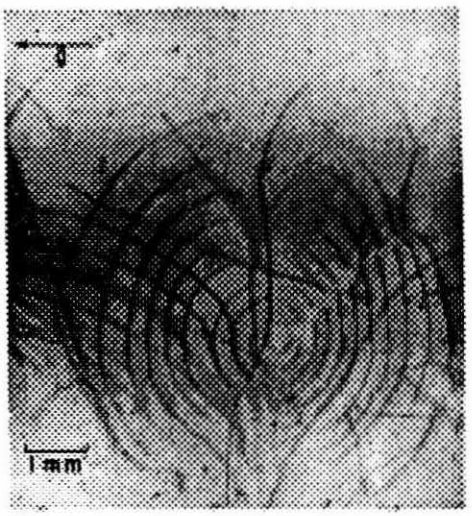

Figure 7. Topograph projected on the (0001) *plane showing concentric dislocation loops in an as-grown crystal of ice. The variation of contrast round the loop is an indication of its prismatic character. The other dislocations seen are typical of the low-density random network in a good as-grown crystal (from Oguro 1988, used with permission of Hokkaido University Press).*

Figure 8 is a topograph showing dislocations projected on the basal plane in a crystal that had been subjected to a compressive stress in a vertical direction (Ahmad and Whitworth 1988). Features with 120° angles as at A and B are dislocations gliding on the basal plane. These dislocations glide as almost straight segments in the screw and 60° orientations, but the corners rapidly become curved after the stress is removed. Very occasionally, for example in a collapsing loop, basal dislocations in edge orientation have also been seen. The long narrow loops like those at C and D have basal Burgers vectors parallel to their lengths and lie on nonbasal planes oblique to the plane of the topo-

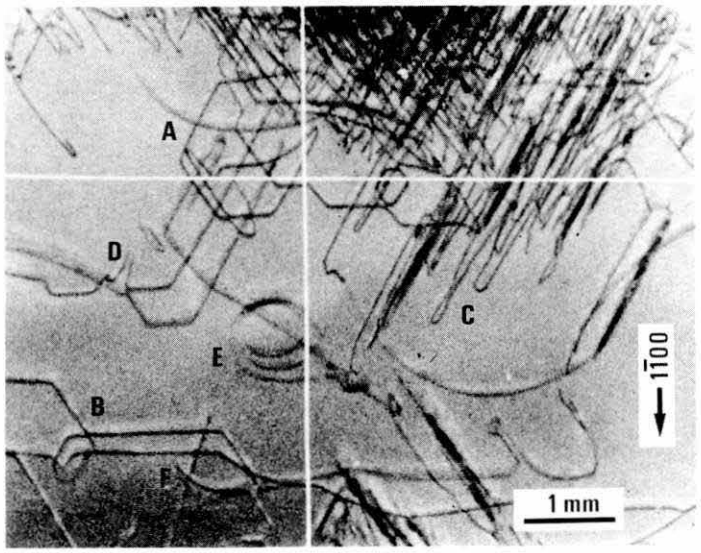

Figure 8. Topograph projected on the (0001) *plane showing dislocations introduced by a compressive stress producing a shear stress on this plane in the vertical direction. The diffraction vector is* 1$\bar{1}$00; *A and D are loops in the basal plane. C and D show edge dislocation segments on nonbasal planes lying oblique to the plane of the topograph, which are dragging long screw dislocations behind them. E is a prismatic loop of the kind shown in Figure 7 (from Ahmad and Whitworth 1988).*

graph. The tip of the loop is an edge dislocation on the nonbasal plane, and the long segments in the figure are screw dislocations. The loop E is a prismatic loop of the type shown in Figure 7.

Similar features to the nonbasal loops at C and D have been reported in the work of Fukuda et al. (1987) (see also Fukuda and Higashi 1988), but the nature of this nonbasal glide is best revealed in crystals stressed parallel to the basal plane, as shown in Figure 9 (Shearwood and Whitworth 1989). This shows dislocations propagating from a scratch on the back surface of a crystal with the orientation shown; the edge dislocations move on {$\bar{1}$010} planes, but the screw dislocations that they leave behind do not glide on these planes. The separation of the screw segments of loops, such as

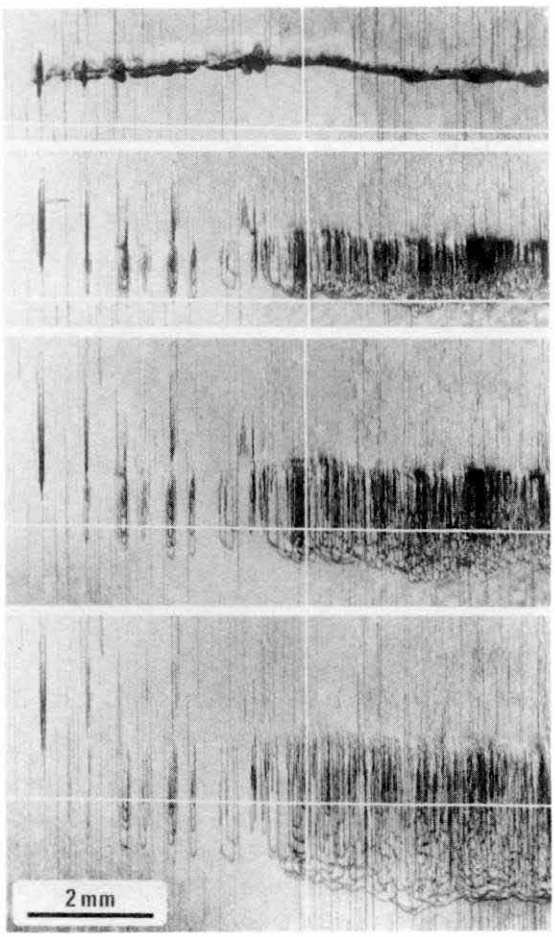

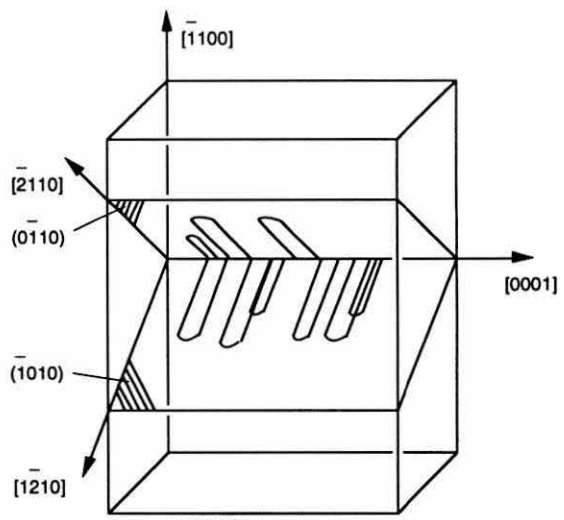

Figure 9. Sequence of topographs (left) showing edge dislocations propagating on the (0$\bar{1}$10) *and* ($\bar{1}$010) *planes from a scratch on the surface of a crystal oriented as indicated above to prevent basal slip (from Shearwood and Whitworth 1989, reproduced courtesy of the International Glaciological Society from* Journal of Glaciology, *35(120): 202).*

C in Figure 8, arises from glide on the basal plane. Hondoh et al. (1990) have also studied nonbasal slip in specimens with the [0001] axis perpendicular to the stress.

We conclude from these observations that all glide dislocations have Burgers vectors in the basal plane, and that loops expanding on this plane take up a hexagonal form made up of screw and 60° segments. The screw segments cannot cross-glide on nonbasal planes, but edge dislocations can glide easily on nonbasal planes containing their Burgers vector. These characteristics are probably unique to ice, and are relevant to its high degree of plastic anisotropy.

DISLOCATION MOBILITY

Experimental observations

The most detailed measurements of dislocation velocities are those of Shearwood and Whitworth (1991), who obtained sequences of topographs showing the positions of dislocations between successive applications of stress. Figure 10 shows tracings of such positions for a loop expanding on the basal plane, and Figure 11 shows the projection on the basal plane of an edge dislocation moving to the lower left on a nonbasal plane. For the stresses up to 1 MPa used in these experiments, the dislocation velocity v_d was found to be directly proportional to stress τ; the velocities per unit stress for basal screw, basal 60° and nonbasal edge dislocations in pure ice are plotted as functions of temper-

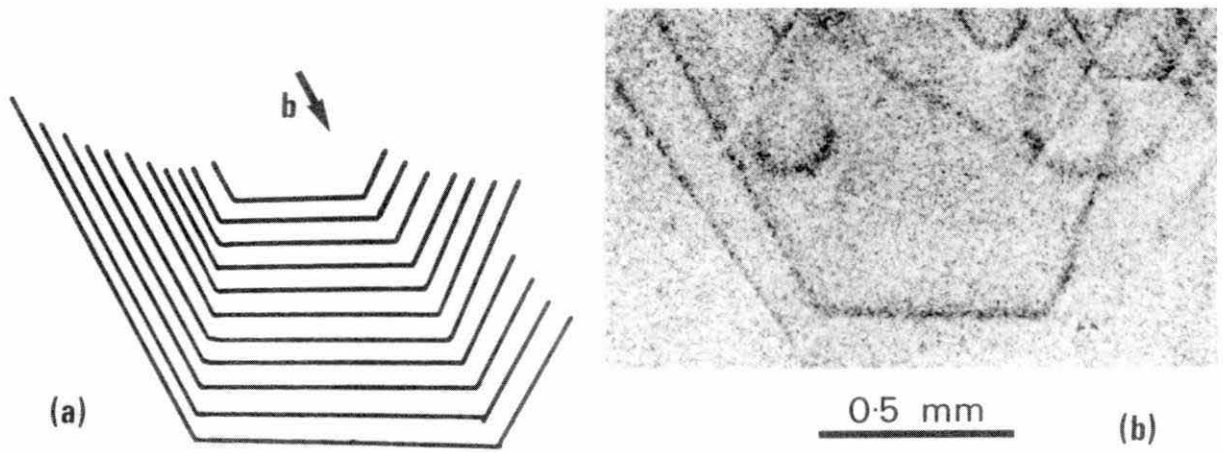

a. Tracings of the positions of the loop. *b. Topographic image traced as the sixth line in Figure 10a.*

Figure 10. Hexagonal dislocation loop expanding on the (0001) plane after successive loadings (from Shearwood and Whitworth 1991).

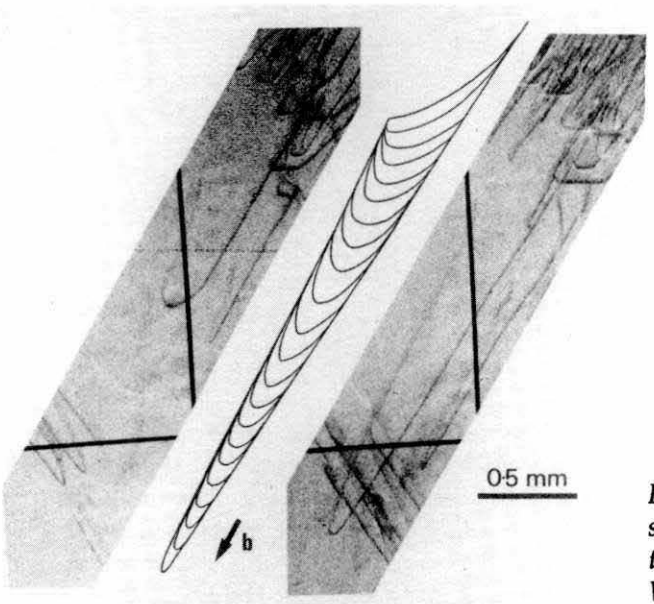

Figure 11. Two topographs and a sequence of tracings showing the motion of a pointed dislocation loop gliding to lower left on a nonbasal plane (from Shearwood and Whitworth 1991).

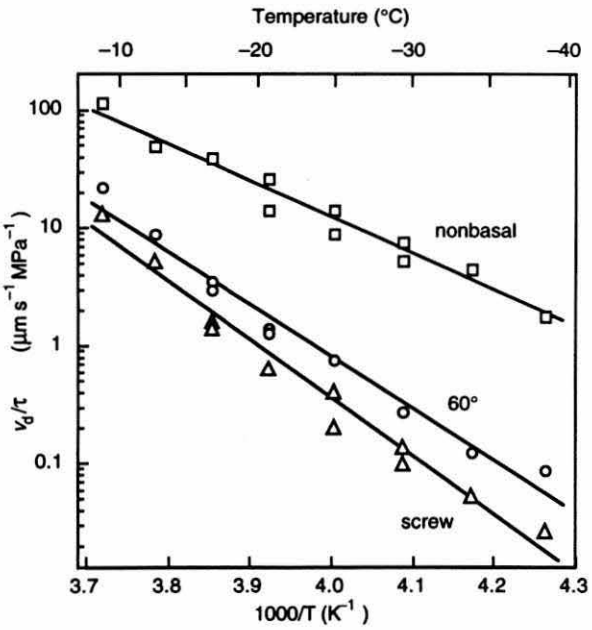

Figure 12. Dislocation velocities per unit stress v_d/τ in pure ice as functions of inverse temperature 1/T for screw and 60° dislocation segments on the basal plane and for edge segments on nonbasal planes (after Shearwood and Whitworth 1991).

ature in Figure 12. The results for nonbasal dislocations are consistent with the observations of Hondoh et al. (1990). Earlier results, such as those of Yamamoto and Fukuda (quoted by Fukuda et al. 1987) and Maï (1976), do not distinguish among different types of dislocations, and were probably subject to recovery in the time taken to obtain the topographs. There is no evidence to support the nonlinear dependence of velocity on stress reported by Maï.

In so far as the Arrhenius plots in Figure 12 are straight lines, the activation energies for dislocation glide (actually from plots of $\ln(v_d T/\tau)$ vs. $1/T$) are as in Table 1.

Another technique, which in principle provides information about dislocation mobility, is internal friction. Many experiments (e.g., Vassoille et al. 1978, Tatibouet et al. 1986) have observed a contribution that increases with temperature, is enhanced by plastic deformation and often depends on amplitude. This effect can reliably be attributed to dislocations and might be usable for distinguishing among the motion of kinks, the nucleation of kinks and breakaway from pinning points, but there are too many disposable parameters for us to draw conclusions from the observations.

Table 1. Activation energies for glide of dislocations in pure ice (after Shearwood and Whitworth 1991).

	Activation energy (eV)
Basal screw	0.95 ± 0.05
Basal 60°	0.87 ± 0.04
Nonbasal edge	0.63 ± 0.04

Peierls model for basal dislocations

The fact that, under stress, dislocations on the basal plane glide quickly into hexagonal form and then glide as straight segments is strong evidence for motion across a Peierls barrier, as is also observed in materials such as silicon (George and Rabier 1987, Nadgornyi 1988). The energy of a dislocation will be minimized when it lies along a particular line in the crystal lattice, and a step on the dislocation between two such lines constitutes a kink, as in Figures 4 and 5. The kinks can glide along the dislocation, and under stress their motion will carry the dislocation forward until it consists of almost straight segments along the directions of minimum energy. In ice these are the screw and 60° segments seen in Figure 10. To advance further, double kinks must be thrown forward across the Peierls barrier and then move sideways until they reach the end of the segment or are annihilated by other kinks. A computer simulation illustrating this behavior is shown in Figure 13. The dislocation velocity is given by

$$v_d = h n_k v_k \qquad (1)$$

where n_k = number of kinks per unit length

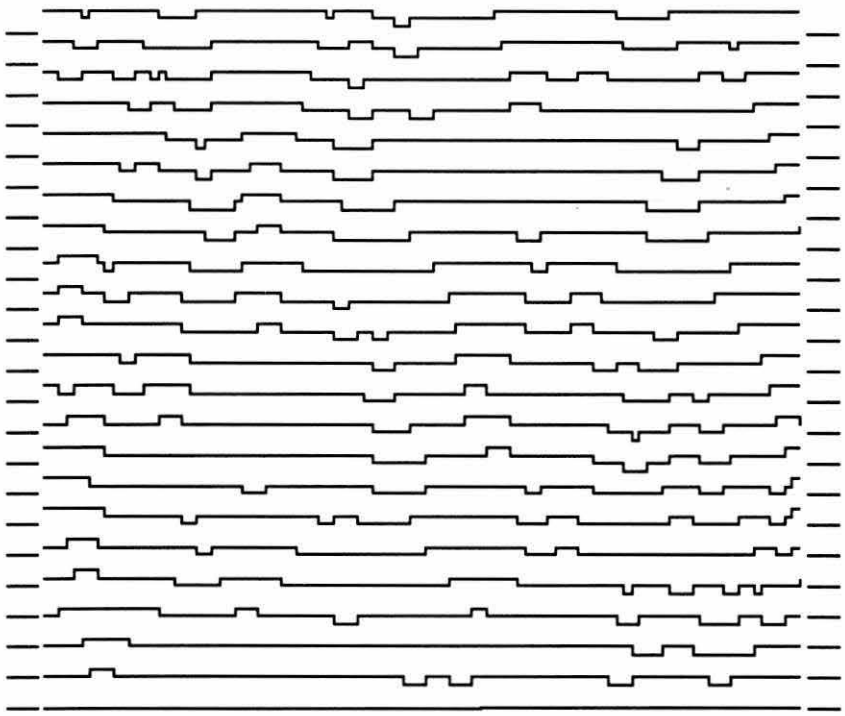

Figure 13. Computer simulation of glide of a dislocation across a Peierls barrier by the nucleation of kink pairs and by the glide of the kinks along the dislocation. The dislocation is gliding upwards in the figure and successive positions are shown above one another. The original position for each case is indicated by the marks at the edges of the diagram.

v_k = their velocity
h = separation of the Peierls troughs.

According to the standard theory of this kind of dislocation motion (Hirth and Lothe 1982), in the limit of low stress ($\tau bah \ll k_B T$, where a is the lattice parameter and b is the Burgers vector), v_d is linearly proportional to stress. It depends on both the activation free energy to form an isolated kink F_k and that to move it F_m according to the equation

$$v_d = \nu \frac{2\tau b a h^2}{k_B T} \exp\left[-\frac{F_k + F_m}{k_B T}\right]. \qquad (2)$$

The quantity ν is a characteristic frequency that cannot be more than the Debye cutoff frequency. The free energy F_k can be written in terms of the energies and entropies of formation $[E_k(T) - TS_k]$, and the measured activation energy for glide is the temperature independent part of $(E_k + E_m)$. However, with the above experimental values and other known parameters, the entropies of activation turn out to be remarkably high (for details see Shearwood and Whitworth 1991). This model indicates that dislocations seem able to move more easily than expected. The contributions arising from kink nucleation and kink migration can in principle be separated by studying the motion of curved segments (Hondoh 1992), but this has not yet been successfully achieved.

Proton disorder

A unique feature of ice, first recognized by Glen (1968), is that the disorder of the protons presents in principle an obstacle to the glide of dislocations. This arises quite simply, because, if two planes of molecules are linked by randomly oriented hydrogen bonds, they cannot be sheared over one another and still link up correctly. The idea is easily understood by considering a 60° dislocation on planes of the shuffle set as shown in Figure 14, where the positions of the protons are disordered. For the dislocation to glide to the left, bond DD' must be broken and D' joined to C. This presents no problem, but for motion to the right, C must link to C', which would create a D-defect. There is not sufficient energy from the stress to create this defect, and there is in general no local rearrangement of bonds that will avoid the formation of a defect somewhere. In practice we expect glide to

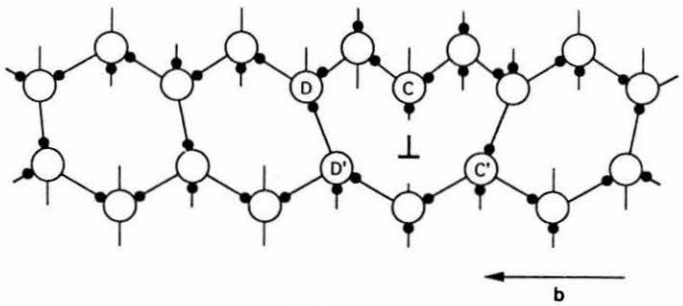

Figure 14. Section in the $(1\bar{1}00)$ *plane of a 60° dislocation on a plane of the shuffle set in the structure of ice, illustrating the consequence of the disorder of the protons according to the model of Glen (1968).*

occur by the motion of kinks along the dislocation, with each step of the kink involving a single exchange of bonds like the one just considered. There will be a 50% chance of the bonds being mismatched at each step.

Glen therefore proposed that the rate-limiting step for dislocation motion may be the rate at which bonds are randomly reoriented by ions or Bjerrum defects, as in the process of dielectric relaxation. It is important to realize that the stress cannot force the reorientation of the required bonds as the dislocation approaches. This idea was quantified for kinks on the shuffle plane by Whitworth et al. (1976) and Frost et al. (1976). The stresses involved are always such that they impose a small bias on the random motion of the kinks; the kinks are not pushed up against the mismatched bonds. With this assumption, the kink velocity v_k for reorientations by Bjerrum defects is given by

$$v_k = \frac{6\sqrt{3}a^4}{2\tau_b k_B T}\,\tau \qquad (3)$$

where τ_b is the mean time to reorient a bond.

For dislocations on planes of the glide set, the obstacle presented by proton disorder may be less severe. Provided the core is not reconstructed, molecules B and C in Figures 5a and b are free to rotate about the single bond, perpendicular to the glide plane, as they switch their linkages from G and H to A and D. For a kink on an unreconstructed partial dislocation, Whitworth (1980) showed that

$$v_k = \frac{1240\sqrt{3}a^4}{4\tau_b k_B T}\,\tau. \qquad (4)$$

If the partial dislocation is reconstructed, the barrier presented by proton disorder will be much greater, but this situation has not been analyzed theoretically. In all cases where a Peierls barrier is present, proton disorder will affect the rate of kink nucleation as well as the kink mobility, but it can only make the theoretical velocity less than that predicted from eq 2. A theory has also been developed for a flexible dislocation line (Whitworth 1983). This does not seem to be applicable to dislocations that glide as straight segments, but may be applicable for nonbasal edge dislocations.

The quantity τ_b is the mean time for the reorientation of bonds close to the dislocation core, and, if we assume that the ice rules are applicable, this will take place by the motion of Bjerrum defects or ions. In bulk crystal, this time is approximately the same as the Debye relaxation time τ_D, but Shearwood and Whitworth (1991) have shown that, for dislocations to move at the observed rate, the appropriate value of τ_b must be much shorter than this. A critical experiment to establish the possible relation of the dislocation velocity to the bond reorientation rate in bulk ice is to measure velocities in doped ice. This was first attempted for HF doping by Maï et al. (1978), who found a small effect, but much less than predicted. Using HCl doping, Shearwood and Whitworth (1992) found no significant effect under conditions where τ_D was known to have been reduced by more than a factor of 10.

From all that we know about the disorder of the protons in ice, it is essential that there be a process for the reorientation of bonds at the dislocation core that retains compatibility with the ice rules in the surrounding material. It could arise from an enhanced concentration or mobility of ions or Bjerrum defects near the core. Interstitials or vacancies should not be directly involved as they do not change the proton disorder. Perez et al. (1978, 1980) postulated that the dislocation core was in some sense noncrystalline, thereby avoiding the

obstacle presented by the ice rules. Their particular model has several adjustable parameters, and these take unphysical values that depend on the nonlinearity in their observations of $v_d(\tau)$. The fact that dislocations glide as straight segments in crystalline orientations indicates that the core must retain much of its crystalline character. The precise way in which dislocations overcome the barrier presented by proton disorder is at present unknown, and, as we will see in the *Doped Crystals and Electrical Effects* section, there is conflicting evidence about whether proton disorder is rate limiting.

There is no evidence for a Peierls barrier to the motion of nonbasal edge dislocations, and this is consistent with their having a lower activation energy for glide. However, the limitations presented by proton disorder are in principle equally important in this case (Whitworth 1983, Shearwood and Whitworth 1991). The most significant fact about nonbasal slip is the complete absence of any glide of screw dislocations on the nonbasal planes at the stresses used. This is strong evidence that the screw dislocations are dissociated into partial dislocations on the basal plane, and provides circumstantial evidence for basal slip being between planes of the glide set.

Weertman (1963) proposed a further mechanism by which the disorder of the protons in ice will inhibit the motion of dislocations: anelastic loss, which arises from reorientation of molecules in the stress field of the dislocation as it moves. Any such effect will constitute a barrier additional to those already considered, and seems likely to be comparatively small.

ROLE OF DISLOCATIONS IN PLASTIC DEFORMATION OF SINGLE CRYSTALS

Pure crystals

For the plastic deformation of a crystal on a single slip system, the strain rate $\dot{\varepsilon}$ is given by the equation

$$\dot{\varepsilon} = \phi N_d b v_d \qquad (5)$$

where N_d = density of mobile dislocations (length per unit volume)
b = Burgers vector
v_d = dislocation velocity
ϕ = factor depending on the orientation of the slip system.

If several slip systems operate together, their contributions to the strain rate must be summed. Crystals of ice normally deform almost exclusively on the basal plane, and Figure 15 shows the form of the stress–strain curve for such deformation in constant strain rate tensile tests (Higashi et al. 1964). The peak followed by a yield drop arises because N_d is initially small and the constant deformation rate requires a high value of v_d, but as N_d increases during the deformation, the stress necessary to maintain a smaller v_d becomes smaller. Eventually, deformation may proceed at constant stress. There is little work-hardening in ice, and in the steady-state region there will be a balance among dislocation multiplication, emergence from the surface and recovery processes.

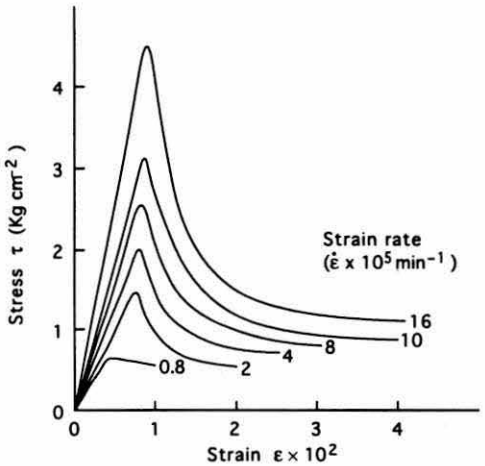

Figure 15. Stress–strain curves for tensile deformation of single crystals of ice at –15°C and at the constant strain rates shown (after Higashi et al. 1964).

The corresponding behavior to Figure 15 in a creep test at constant stress would be an initially accelerating creep leading to a constant strain rate. Higashi et al. (1965) have reported this kind of creep in a very special bending geometry, but in tensile tests continuously accelerating creep is observed, for which $\varepsilon \propto t^m$ with $m \approx 1.5$ to 2. The macroscopic deformation of ice depends critically on the initial state of the crystal and the conditions of the experiment, but results are generally fitted to the empirical equation

$$\dot{\varepsilon} \propto \sigma^n \exp(-E/k_B T) \qquad (6)$$

where for single crystals $n \approx 2$. There is some difficulty in determining a value for the activation energy E, because values deduced from constant-strain-rate tests depend on the value of n, while strictly comparable conditions are difficult to achieve in creep tests at different temperatures.

Table 2. Activation energies for plastic deformation of single crystals of ice at temperatures of –10 to –50°C.

Type of deformation	*Activation energy E (eV)*	*Reference*
Tensile–constant $\dot{\varepsilon}$	0.68	Higashi et al. (1964)
Tensile–constant ε	0.62	Readey and Kingery (1964)
Bending creep	0.68	Higashi et al. (1965)
Tensile creep	0.68	Jones and Glen (1969a)
Tensile creep	0.80	Homer and Glen (1978)
Tensile creep	0.62	Ramseier (unpublished)*

* From Weertman (1973).

Table 2 summarizes values deduced by different authors in different ways from tests on single crystals in the range –10 to –50°C. There are many more data on polycrystalline ice, but this deforms very differently and other considerations will be rate limiting. For a detailed review of creep in ice, see Weertman (1973).

The interesting fact that emerges from this table is that the values of E are all less than those in Table 1 for the glide of dislocation segments on the basal plane in this range of temperatures. Extensive studies of silicon reveal no such discrepancy, but it does exist in some other semiconductors (Rabier and George 1987). There are two possible reasons for the difference. Either the dislocation density for steady-state creep increases with falling temperature, or, under deformation conditions, the dislocations do not glide as straight segments. If it is easier to create kinks within the deforming material than under the near-perfect conditions of topography experiments, the activation energy should be reduced. Macroscopic deformation is such a complicated process that it is not surprising that there is considerable variation among experiments.

Crystals oriented with the stress perpendicular to the [0001] axis can be deformed by slip on $\{1\bar{1}00\}$ planes, but this requires a stress of some 50 times that for slip on the basal plane, and after such deformation voids are created in the specimen (Muguruma et al. 1966). We have seen in topographic experiments that edge dislocations move very easily on these nonbasal planes, but screw dislocations were not observed to glide off the basal plane. This means that a dislocation loop that starts to move on a nonbasal plane cannot expand to cover the whole plane; slip will be confined to narrow strips bounded by screw dislocations as seen in Figure 9, and macroscopic slip will be very difficult. Hondoh et al. (1990) reproduce a figure showing that such slip is associated with very short slip lines, which correspond well with this interpretation.

To produce macroscopic deformation, it is not sufficient that dislocations should glide. There have to be processes by which dislocations can multiply on their slip plane and by which slip can be transferred from one slip plane to another. The standard mechanism is the Frank-Read source (see Read 1953). An example of such a source is illustrated in Figure 16a, in which dislocation segments spiral around a fixed point where the dislocation makes a step from one glide plane to another. Ahmad et al. (1986) observed such a source in topographic experiments on ice, and Figure 17 shows an example. In normal materials many such sources are generated by the cross slip of screw dislocations off their primary glide planes, but the immobility of screw dislocations on the nonbasal planes in ice means that this does not occur. However, a feature of ice is the high mobility of edge segments on nonbasal planes, and this means that the segment S, which acts as the fixed center of the Frank-Read action in Figure 16a, may not remain fixed but more often glides away from the original dislocation, trailing screw segments behind it as shown in Figure 16b. This leads to features such as

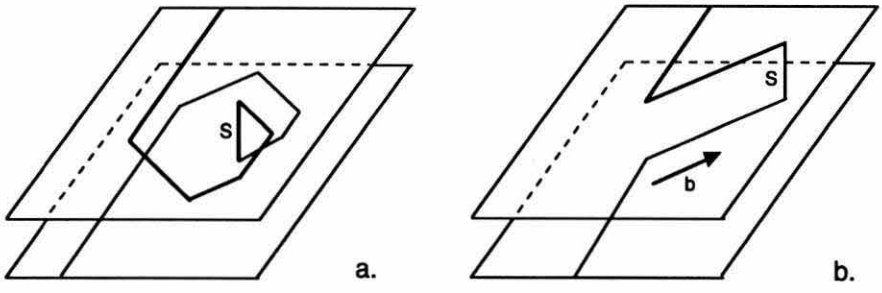

Figure 16. Operation of a Frank-Read source on the basal plane (a), and what happens in ice if the linking segment S does not remain fixed but glides rapidly on the nonbasal slip plane (b).

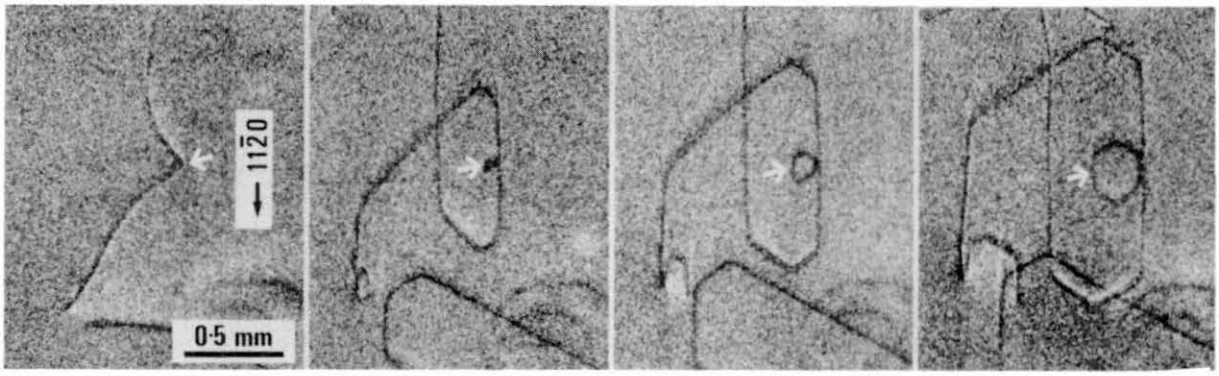

Figure 17. Sequence of topographs projected on the (0001) *plane showing operation of a Frank-Read source in ice. This corresponds to Figure 16a (from Ahmad et al. 1992, used with permission of Hokkaido University Press).*

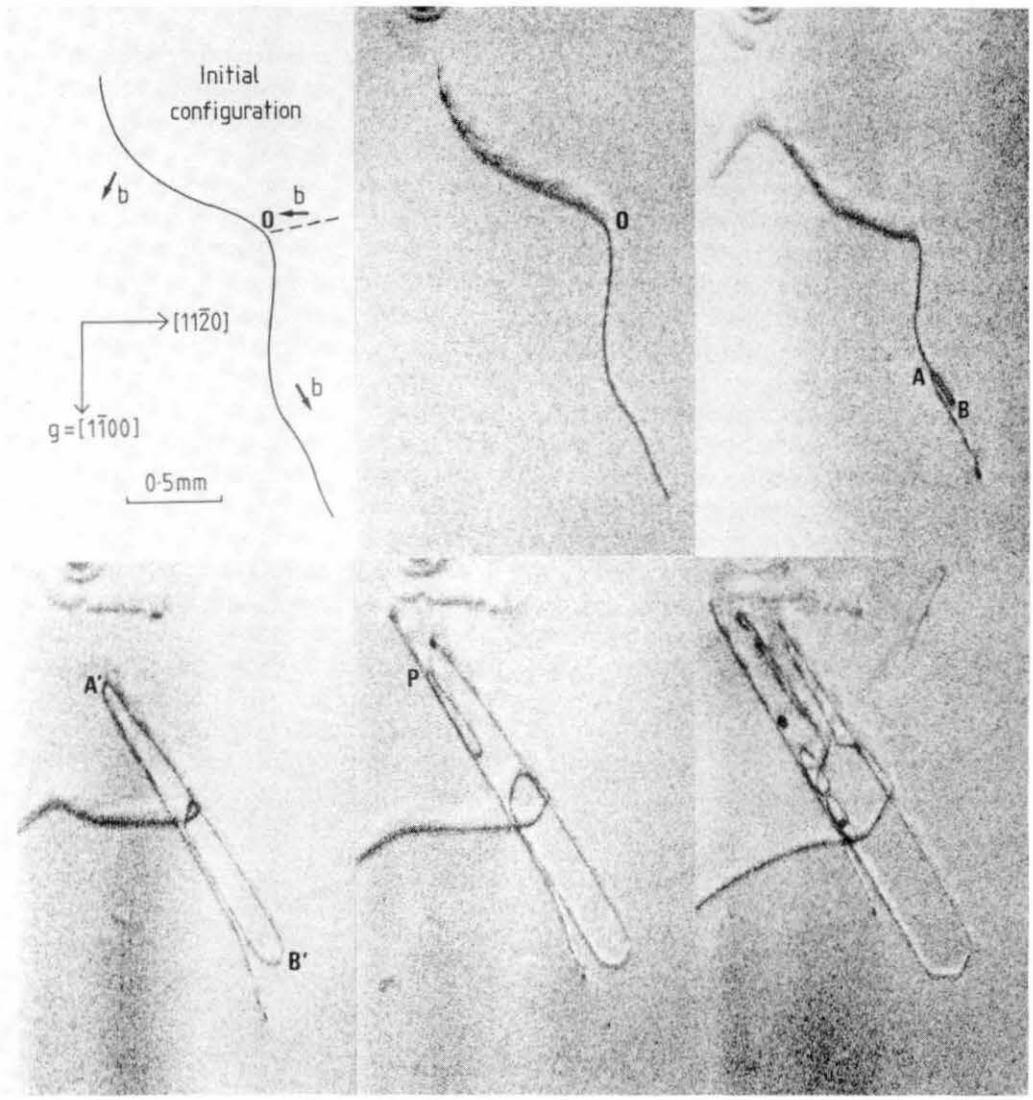

Figure 18. Sequence of topographs projected on the (0001) *plane showing dislocation multiplication arising from the fast edge segments such as A on a nonbasal plane oblique to the plane of the figure. The section at B, which develops hexagonal features, is on the basal plane and glides more slowly. In the last two topographs the dislocation loops have cut the surface at upper left (from Ahmad et al. 1992, used with permission of Hokkaido University Press).*

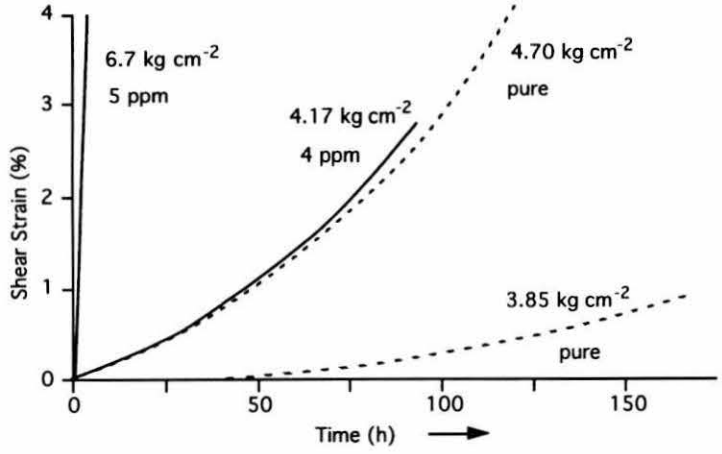

a. Creep curves.

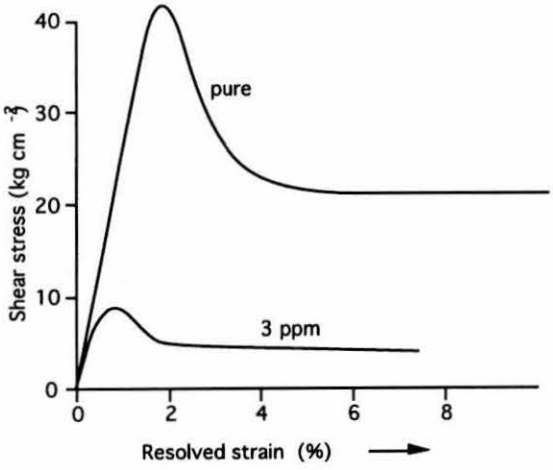

b. Constant-strain-rate tests.

Figure 19. Test results from pure single crystals of ice and crystals doped with HF at the concentrations given. Temperature is –70°C (after Jones 1967).

C in Figure 8 and to multiplication of the kind shown in Figure 18. The behavior of nonbasal edge dislocations that cut the surface is also very significant (Ahmad et al. 1992, Shearwood and Whitworth 1993).

Doped crystals and electrical effects

Jones and Glen (1969b) found that doping ice with HF produced a remarkable softening in both creep tests and constant-strain-rate tests at –60 to –70°C (Fig. 19). The softening was observed both in crystals doped before deformation and when HF was diffused into the specimen part way through the test. NH_4OH produced a small hardening. Nakamura and Jones (1970) deformed HCl-doped ice, but at higher temperatures, and observed a softening, though the effect was much less than with HF. All of these observations indicate a strong correlation in the effects of the dopant on the deformation rate and on the rate of bond reorientation as observed in dielectric experiments. This led to Glen's (1968) hypothesis that proton disorder is the rate limiting process for dislocation glide.

The topographic observations of Shearwood and Whitworth (1992) showed no effect of HCl doping on the mobility of dislocations at a level of doping that produced a ten-fold decrease in τ_D, but this doping was very much less than that which gave the large effects observed by Jones and Glen. A further complication is that strain rate depends on the product of dislocation density and dislocation velocity, and Jones and Gilra (1972) found that diffusing HF into ice, as was done in some of the experiments referred to, produced a large increase in dislocation density.

An alternative way of changing the concentrations of point defects that gives rise to bond reorientation is the application of an electric field (Petrenko and Schulson 1992). By applying electric fields to thin specimens undergoing deformation

in shear, Petrenko and Schulson (1993) have shown that a reduction in the high-frequency conductivity leads to a corresponding reduction in creep rate. We have already seen that dislocation glide involves the reorientation of bonds near the core. There is considerable evidence that under certain conditions changing the bond reorientation rate in the bulk of the crystal can have an effect on the dislocation mobility.

Different kinds of electrical effects can arise if the dislocations carry a net charge. Such a charge is to be expected where there are dangling bonds, because the numbers of bonds with and without protons do not have to be equal. In equilibrium any such charge will be screened by a surrounding cloud of excess electrical point defects of opposite sign (see Whitworth 1975), but during deformation a dislocation may become separated from this charge cloud. Petrenko and Whitworth (1983) observed small transverse electric currents associated with the tensile deformation of previously bent crystals, and interpreted them as ascribable to dislocations carrying a net positive charge of at least 0.002 protonic charges per atomic length. Itagaki (1970) has reported X-ray topographic experiments in which dislocations appear to move in an alternating electric field. In cases where the sign of the charge could be identified, it was positive, but it is difficult to deduce magnitudes from such experiments. A problem with any experiment of this kind is that the field should be maintained for a sufficient time to move the dislocations by an observable amount, but in this time the field is largely eliminated by polarization and conduction in the ice. If the dislocation cores are indeed reconstructed, as suggested in the *Basal Dislocations* section, then any core charge will be confined to kink sites or perhaps to Bjerrum type defects trapped in the reconstruction.

STACKING FAULTS

Structure of stacking faults in ice

The crystal structure of ice consists of (0001) planes of molecules stacked above one another as illustrated in Figure 2. If the positions of these layers in their planes are denoted by the letters A,B,C, as defined in Figure 3, the hexagonal structure of ice I_h follows the sequence

AABBAABBAABB....

The C positions are unoccupied, resulting in empty channels running through the structure in the [0001] direction. Stacking faults arise if the stacking across the planes marked "glide" in Figure 2 departs from the perfect sequence. For a general discussion of such faults, the reader is referred to Hirth and Lothe (1982) or a similar text. To simplify the discussion, we will denote each pair of layers such as AA by the single letter A, and the stack-ing is then that familiar in hexagonal close packing

ABABABAB....

Cubic ice (ice I_c) has the stacking

ABCABCABC...

but is energetically unstable relative to ice I_h.

A stacking fault is a planar defect normally lying on a (0001) plane of the glide set. It must extend to the surface or terminate at a partial dislocation with a Burgers vector equal to the displacement required to create the fault. To distinguish among the possible kinds of faults, it is useful to introduce Frank's notation, which concentrates not on the absolute location of the layers A,B,C but only on the stacking relative to the layer below. Thus, the equivalent stackings of B on A, C on B and A on C are all denoted by the symbol Δ, while the inverse stacking of A on B, B on C or C on A are given the symbol ∇. The hexagonal stackings ABABAB..., BCBCBC... or CACACA... are then all denoted by

$\Delta\nabla\Delta\nabla\Delta\nabla\Delta\nabla\ldots$

whereas cubic stacking would be

$\Delta\Delta\Delta\Delta\Delta\Delta\Delta\Delta\ldots$ or $\nabla\nabla\nabla\nabla\nabla\nabla\nabla\nabla\ldots$.

There are four simple ways of introducing stacking faults into ice, and these are illustrated in Figure 20. The first is to shear a B layer over an A layer into a C position. This changes a Δ into a ∇ giving the fault

$$\begin{array}{l} \downarrow \\ \text{BABACBCB}\ldots \\ \nabla\Delta\nabla\nabla\Delta\nabla \end{array}$$

This fault is illustrated in Figure 20a, in which it terminates in a partial dislocation of the Burgers vector $(a/3)\langle 10\bar{1}0\rangle$. When a perfect $(a/3)\langle 11\bar{2}0\rangle$ dislocation dissociates into two Shockley partial dislocations on a (0001) plane of the glide set, according to the equation

$$(a/3)\langle 11\bar{2}0\rangle \rightarrow (a/3)\langle 10\bar{1}0\rangle + (a/3)\langle 01\bar{1}0\rangle$$

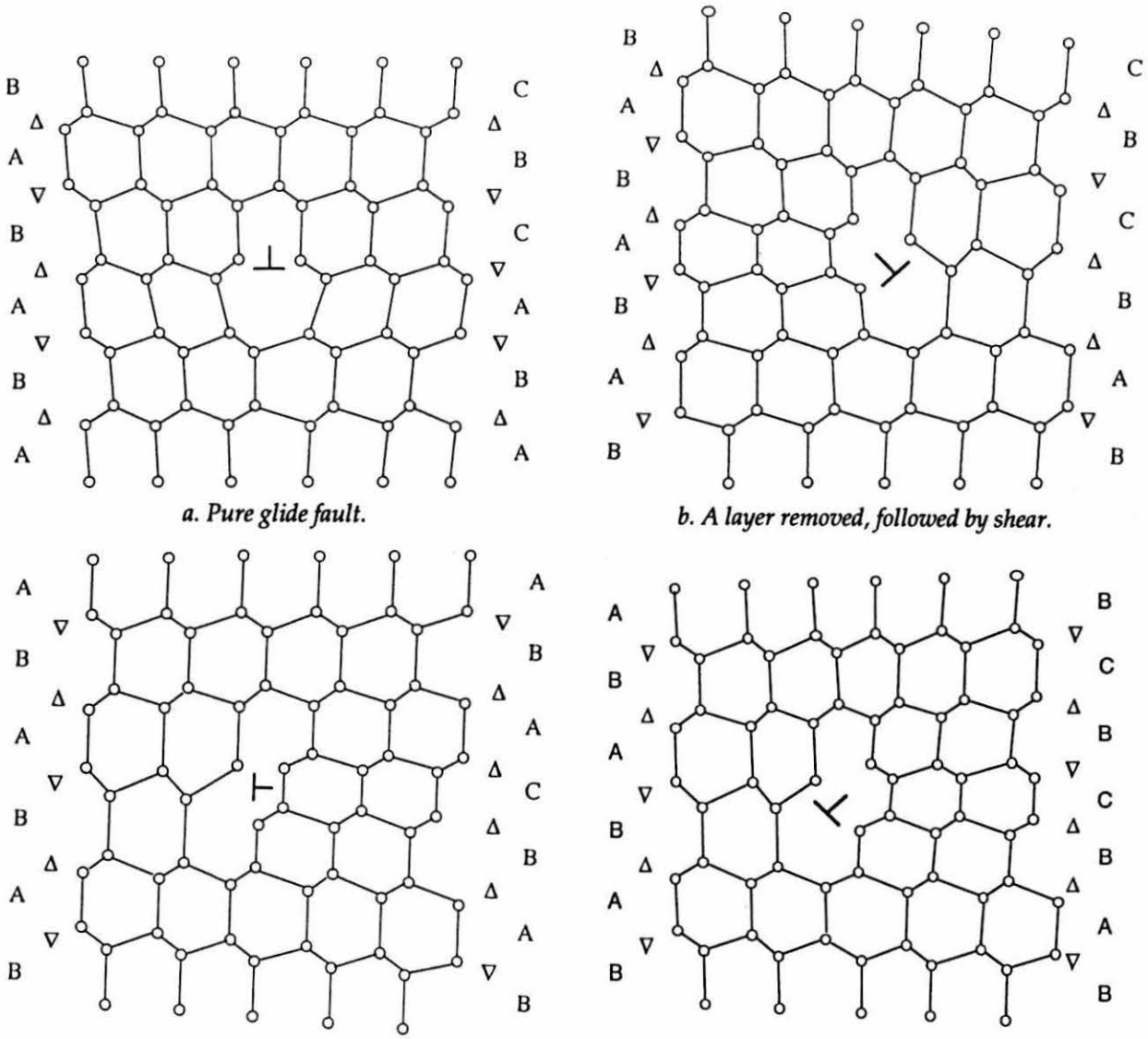

a. Pure glide fault.

b. A layer removed, followed by shear.

c. C layer added.

d. C layer added followed by shear above the added layer.

Figure 20. Projections of structure of ice I_h on a $(1\bar{2}10)$ plane showing stacking faults in the right-hand portion of each diagram terminating at an appropriate dislocation in the center.

as described in the *Basal Dislocations* section, this is the type of stacking fault ribbon that will be formed between them.

The other types of faults require the addition or removal of a layer A, B or C, which consists of two planes of molecules. If an A layer is removed, the B layers on opposite sides of it can only link together if there is a displacement of one-half of the crystal over the other by an amount $(a/3) < 10\bar{1}0>$, generating the fault

↓

ABABCBCB...

∇Δ∇∇∇Δ∇

This fault is shown in Figure 20b. The dislocation surrounding it has both prismatic and glide components, and its Burgers vector is $(1/6) <20\bar{2}3>$.

Unlike the case just described, the addition of a C layer to the perfect ABAB... structure does not necessitate any shear, and the fault generated is

↓

ABABCABCB...

Δ∇Δ**Δ**Δ∇Δ

This fault is illustrated in Figure 20c; it is surrounded by a prismatic dislocation loop of Burgers vector $(c/2)$ [0001]. The fault contains four

consecutive Δ-type stackings, which resembles cubic ice. It can lower its energy by a shear between the C and the A layer at the point marked ↓, yielding the fault

↓
ABABCBCBC...
ΔV∆∆V∆V∆

which is shown in Figure 20d. Examination of the ΔV sequence shows that this is the same stacking as in Figure 20b, but the nature of the bounding dislocation corresponds to an interstitial rather than a vacancy-type prismatic loop. Stacking faults are often classified as *intrinsic* if perfect stacking is maintained up to the plane of the fault and *extrinsic* if it is not; on this basis the faults of Figures 20a, b and d are intrinsic and only the higher energy fault 20c is extrinsic.

Observations of stacking faults

Stacking faults of macroscopic dimensions can be observed by X-ray topography and have been studied extensively in ice by the group at Sapporo. Their work is reviewed by Fukuda et al. (1987), Oguro and Hondoh (1988) and Oguro et al. (1988). Stacking faults in ice are energetically unstable and never remain in crystals that have been well annealed and observed at the temperature of annealing. However, a few large-area faults do occur in freshly grown crystals (Hondoh et al. 1983), and their formation is enhanced by doping, particularly with NH_3 (Oguro and Higashi 1973).

Figure 21 is an example of a topograph of pure ice cooled to –45°C. The dark areas correspond to stacking faults parallel to the basal plane. The large, irregular faults originate from the growth of the crystal, while the smaller patches are prismatic loops formed during cooling. The presence of contrast within the area of the fault shows that the fault vector **f** satisfies the condition $\mathbf{g}\cdot\mathbf{f} \neq 0$ or an integer, where **g** is the diffraction vector of the topograph. With $\mathbf{g} = <10\bar{1}0>$ this means that the faults must have a shear component. The bounding dislocations have a [0001] component, and careful analysis shows that the faulted loops formed on cooling are

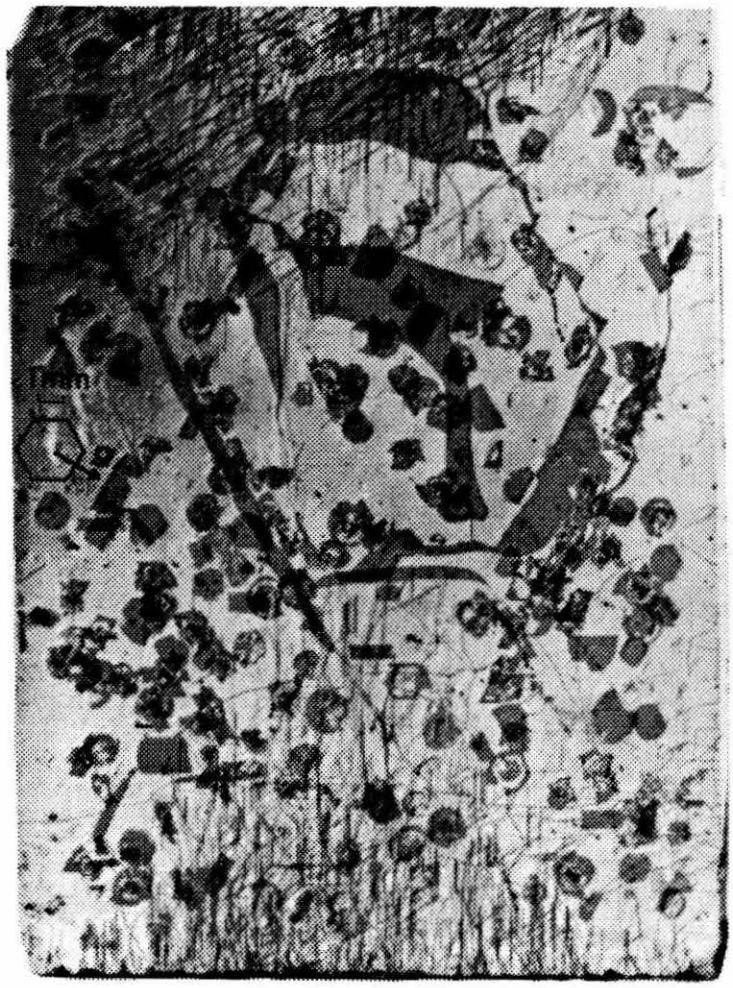

Figure 21. X-ray topograph projected on a (0001) *plane of a crystal of pure ice cooled rapidly to –45°C, resulting in the production of faulted prismatic dislocation loops by the condensation of interstitials (from Oguro et al. 1988, used with permission of Hokkaido University Press).*

interstitial in character (Hondoh at al. 1983). It appears that an interstitial loop with the Burgers vector $(c/2)$ [0001] does in fact lower its energy by taking the sheared form of Figure 20d rather than that of Figure 20c. The stable prismatic loops shown in Figure 7 are presumably perfect dislocations, with the Burgers vector c[0001] including two double layers of molecules within the loop; such dislocations will have high energy and will almost certainly be dissociated, but the stacking fault ribbon between them is unresolvable in topography.

As described in Volume 1, *Point Defects* (Petrenko and Whitworth [1994], see section on *Molecular Defects*), very detailed studies of the growth and shrinkage of faulted and unfaulted dislocation loops have yielded the best available parameters for the formation and self-diffusion of interstitials in ice (Goto et al. 1986, Hondoh 1992). The energy of a $(1/6) <20\bar{2}3>$ fault has been determined to be 0.31 mJ m^{-2}, which is 3×10^{-4} eV per molecule in the plane. This is assumed to be the lowest energy type of fault because it has only two adjacent Δ's in the stacking sequence. The shear fault with three Δ's is estimated to have twice this energy, and on this basis the separation of the Shockley partial dislocations formed by the dissociation of a perfect $(a/3)$ $<11\bar{2}0>$ dislocation on a basal plane has been estimated by Hondoh et al. (1983) to be 20 nm for a screw dislocation and 46 nm for an edge dislocation. Observation of such dissociation requires electron microscopy and has not yet been achieved in ice.

GRAIN BOUNDARIES

Structure

Natural ice is polycrystalline and the boundaries between the individual crystals (or "grains") can be considered as planar defects within otherwise perfect material. We will briefly describe the intrinsic properties of this class of defects, but will not here consider their role in the macroscopic properties of polycrystalline ice.

Examination of polycrystalline samples shows grains of many shapes, sizes and orientations, depending on the history of the material (e.g., Matsuda and Wakahama 1978). In well-annealed ice, the boundaries are fairly flat, which is a necessary condition for minimizing the surface energy. Within a single grain, or within a piece of ice that is nominally a single crystal, there will often be sub-boundaries, across which there is a lattice misorientation of at most a few degrees and often very much less. These boundaries are made up of arrays of dislocations in accordance with geometrical principles that apply to any crystalline material (see for example Read 1953 or Hirth and Lothe 1982). Except for elastic interactions with one another to form a stable structure, these dislocations behave as individual dislocations within a single crystal. A suitable sub-boundary will migrate by the glide of these dislocations under an appropriately oriented stress, as has been observed in ice by Higashi and Sakai (1961).

For large-angle boundaries, the concept of an array of dislocations is not applicable, and there must be an interface across which the bonding departs greatly from that in a perfect crystal. For some particular orientations, the bonding may be less irregular than for others, and the grain boundary energy will depend on the relative misorientation of the grains and on the location of the boundary between them, as has been observed by Suzuki and Kuroiwa (1972).

A commonly assumed condition for the formation of any special type of low energy boundary is that the lattice points for the two half-crystals should match up with one another in a periodic way along the plane of the boundary. The Coincidence-Site Lattice (CSL) model, which has been described in relation to ice by Higashi (1978) and Hondoh (1988), has this property, but other requirements imposed by the model are not generally thought to be significant (Sutton 1984). A favorable configuration in ice is one in which the grains are rotated relative to one another by 34.1° about the $[10\bar{1}0]$ direction, and such a boundary in which the grains are joined across their $(1\bar{2}11)$ planes is illustrated in Figure 22. Hondoh and Higashi (1978) have grown bicrystals containing this type of boundary and have shown by X-ray topography that the boundary is not flat, but is made up of facets that make small angles to one another. They propose that a facet that makes a small angle to the exact $(1\bar{2}11)$ plane will contain an array of intrinsic grain boundary dislocations of the small Burgers vector shown in Figure 23; between these dislocations the lattices will match exactly as in Figure 22. Experiments on the diffusional motion of boundaries during strain-free annealing have shown variations with the type of boundary and some tendency to form facets with particular orientations (Hondoh and Higashi 1979, Nasello et al. 1992).

Other examples of misorientations that satisfy the CSL conditions are 47° about $[10\bar{1}0]$ and 21.8° about [0001]. The latter is thought to lead to certain types of 12-branched snow flakes (Kobayashi and Furukawa 1975). These special cases can also be

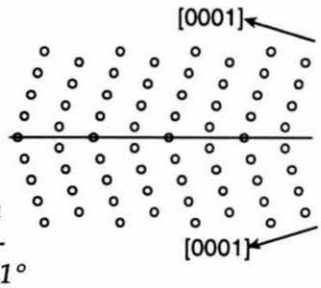

Figure 22. Boundary on a $(1\bar{2}11)$ plane between two grains rotated relative to one another by 34.1° about the $[10\bar{1}0]$ axis perpendicular to the diagram. The circles are lattice points not molecules.

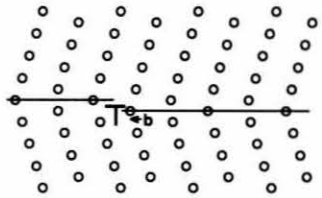

Figure 23. Edge dislocation in the boundary produced by shear in the plane of the boundary by the small Burgers vector shown. This results in the displacement of the boundary downwards in the right-hand part of the diagram.

thought of as growth twins, though in ice they are not usually formed in the ways commonly associated with twinning. It must be remembered that the coincidence of a number of lattice points across an interface does not ensure that hydrogen bonds link up in a manner even approximating that in the perfect crystal, and there must be considerable disorder of the molecules in this region. The thickness of this noncrystalline or 'liquid-like' region is not known. In this connection it is relevant to note that, close to the melting point, liquid water is present in polycrystalline ice in veins that lie along the lines of intersection of grain boundaries (Mader 1992, Nye 1992), and this will be in equilibrium with the internal structure of the boundaries themselves.

Grain boundaries can move in a number of ways, according to principles that are generally applicable to all materials. Under a shear stress a pair of suitably oriented grains may slide over one another on the boundary (Ignat and Frost 1987), but in other cases shear can occur by the migration of the boundary perpendicular to its plane. This has been reported for a 34° $[10\bar{1}0]$ boundary by Hondoh (1988), and explained in terms of the glide of intrinsic boundary dislocations of the type shown in Figure 23.

The motion of grain boundaries, or of dislocations within them, leads to a characteristic peak in the low-frequency internal friction (Perez et al. 1979, Tatibouet et al. 1987). Boundaries also move by diffusive processes in which molecules in one grain are rearranged in the lattice structure of the other, and this is what happens when ice recrystallizes during large-scale plastic flow.

Being places where there are irregularities in the lattice, grain boundaries can act as sources and sinks of point defects and dislocations. We have already referred to the formation of faulted dislocation loops by the condensation of interstitials on cooling. Near a boundary there is a zone where these loops are not formed because the excess interstitials are lost to the boundary (Liu et al., in press). In the very early stages of deformation, stress concentrations form at grain boundaries, and dislocation loops are nucleated from them (Hondoh and Higashi 1983, Liu et al. 1993).

Electrical properties of grain boundaries in doped ice

Electrical measurements on monocrystalline and polycrystalline samples of ice lead to the conclusion that these types of ice differ significantly even when the concentrations of impurities averaged over the volume are the same. As ice does not exhibit any anisotropy of conductivity, we are led to conclude that the grain boundaries make an appreciable contribution to the conductivity.

The most obvious reason why this may be so is that the impurities segregate to the boundaries, and particularly to the triple intersection lines where three grain boundaries meet. Mulvaney et al. (1988) and Wolff et al. (1988) investigated the impurity distribution in polycrystalline Antarctic ice using a scanning electron microscope with a cold stage and an X-ray microanalysis facility with a spatial resolution of 10 nm and a detection limit of 5 mM (equivalent to 490 ppm for H_2SO_4). They found that, although the volume average concentrations were quite small (182 ppb for Na^+, 320 ppb for Cl^-, 764 ppb for SO_4^{2-} and 41 ppb for NO_3^- according to ion-chromatography and atomic absorption spectroscopy), the concentration of SO_4^{2-} at triple junctions was 25 M within an area of 1 m^2. This concentration is close to the eutectic temperature (4.9 M freezing at –73°C), so that such triple junctions remain liquid at very low temperatures and form a network of filaments of extremely high electrical conductivity. Wolff and Paren (1984) have suggested that the d.c. conductivity of polar ice could be caused by the presence of acidic liquid layers at the grain boundaries. They showed that it is plausible that these impurities will concentrate at the triple junctions, and, using reliable data for H_2SO_4, HNO_3 and HCl concentrations at the South Pole, they derived the correct magnitude

and temperature dependence for the conductivity of such ice.

The differences between the electrical properties of monocrystalline and polycrystalline ice seem to persist in nominally pure samples. This suggests that the grain boundaries may have an enhanced conductivity because of the presence of a 'liquid-like' layer, such as has also been proposed for the free surface (see the future report on the *Surface of Ice*). However, at present this is just speculation, and experiments on genuinely pure boundaries will be difficult to achieve.

LITERATURE CITED

Ahmad, S. and R.W. Whitworth (1988) Dislocation motion in ice: A study by synchrotron X-ray topography. *Philosophical Magazine A*, **57**(5): 749–766.

Ahmad, S., M. Ohtomo and R.W. Whitworth (1986) Observation of a dislocation source in ice by synchrotron radiation topography. *Nature*, **319**(6055): 659–660.

Ahmad, S., C. Shearwood and R.W. Whitworth (1992) Dislocation multiplication mechanisms in ice. In *Physics and Chemistry of Ice* (N. Maeno and T. Hondoh, Ed.). Sapporo: Hokkaido University Press, p. 492–496.

Duval, P., M.F. Ashby and I. Anderman (1983) Rate-controlling processes in the creep of polycrystalline ice. *Journal of Physical Chemistry*, **87**(21): 4066–4074.

Falls, A.H., S.T. Wellinghoff, Y. Talmon and E.L. Thomas (1983) A transmission electron microscopy study of hexagonal ice. *Journal of Materials Science*, **18**(9): 2752–2764.

Fletcher, N.H. (1970) *The Chemical Physics of Ice*. Cambridge University Press.

Frost, H.J., D.J. Goodman and M.F. Ashby (1976) Kink velocities on dislocations in ice. A comment on the Whitworth, Paren and Glen model. *Philosophical Magazine*, **33**(6): 951–961.

Fukuda, A. and A. Higashi (1969) X-ray diffraction topographic studies of dislocations in large ice single crystals. *Japanese Journal of Applied Physics*, **8**(8): 993–999.

Fukuda, A. and A. Higashi (1973) Dynamical behaviour of dislocations in ice crystals. *Crystal Lattice Defects*, **4**(3): 203–210.

Fukuda, A. and A. Higashi (1988) Generation, multiplication and motion of dislocations in ice crystals. In *Lattice Defects in Ice Crystals* (A. Higashi, Ed.). Sapporo: Hokkaido University Press, p. 69–96.

Fukuda, A. and H. Shoji (1988) Dislocations in natural ice crystals. In *Lattice Defects in Ice Crystals* (A. Higashi, Ed.). Sapporo: Hokkaido University Press, p. 13–25.

Fukuda, A., T. Hondoh and A. Higashi (1987) Dislocation mechanisms of plastic deformation of ice. *Journal de Physique Colloque C1*, **48**(3): 163–173.

George, A. and J. Rabier (1987) Dislocations and plasticity in semiconductors. I. Dislocation structures and dynamics. *Revue de Physique Appliquée*, **22**(9): 941–966.

Glen, J.W. (1968) The effect of hydrogen disorder on dislocation movement and plastic deformation of ice. *Physik der Kondensierten Materie*, **7**(1): 43–51.

Glen, J.W. (1974) The physics of ice. USA Cold Regions Research and Engineering Laboratory, Monograph MII-C2a.

Glen, J.W. (1975) Mechanics of ice. USA Cold Regions Research and Engineering Laboratory, Monograph MII-C2b.

Glen, J.W. and M.F. Perutz (1954) The growth and deformation of ice crystals. *Journal of Glaciology*, **2**(10): 397–403.

Goto, K., T. Hondoh and A. Higashi (1986) Determination of diffusion coefficients of self-interstitials in ice with a new method of observing climb of dislocations by X-ray topography. *Japanese Journal of Applied Physics*, **25**(3): 351–357.

Heggie, M.I., S.C.P. Maynard and R. Jones (1992) Computer modelling of dislocation glide in ice. In *Physics and Chemistry of Ice* (N. Maeno and T. Hondoh, Ed.). Sapporo: Hokkaido University Press, p. 497–501.

Higashi, A. (1969) Mechanical properties of ice single crystals. In *Physics of Ice* (N. Riehl, B. Bullemer and H. Engelhardt, Ed.). New York: Plenum Press, p. 197–212.

Higashi, A. (1974) Growth and perfection of ice crystals. *Journal of Crystal Growth*, **24/25**: 102–107.

Higashi, A. (1978) Structure and behaviour of grain boundaries in polycrystalline ice. *Journal of Glaciology*, **21**(85): 589–605.

Higashi, A. (Ed.) (1988) *Lattice Defects in Ice Crystals*. Sapporo: Hokkaido University Press.

Higashi, A. and N. Sakai (1961) Movement of small angle boundary of ice crystal. *Journal of the Physical Society of Japan*, **16**(11): 2359–2360.

Higashi, A., S. Koinuma and S. Mae (1964) Plastic yielding in ice single crystals. *Japanese Journal of Applied Physics*, **3**(10): 610–616.

Higashi, A., S. Koinuma and S. Mae (1965) Bending creep in ice single crystals. *Japanese Journal of Applied Physics*, **4**(8): 575-582.

Higashi, A., M. Oguro and A. Fukuda (1968) Growth of ice single crystals from the melt with special

reference to dislocation structure. *Journal of Crystal Growth*, **3/4**: 728–732.

Higuchi, K. (1958) The etching of ice crystals. *Acta Metallurgica*, **6**(10): 636–642.

Hirth, J.P. and J. Lothe (1982) *Theory of Dislocations*, 2nd ed. New York: Wiley.

Hobbs, P.V. (1974) *Ice Physics*. Oxford, United Kingdom: Clarendon Press.

Homer, D.R. and J.W. Glen (1978) The creep activation energy of ice. *Journal of Glaciology*, **21**(85): 429–444.

Hondoh, T. (1988) Observations of large angle grain boundaries in ice crystals. In *Lattice Defects in Ice Crystals* (A. Higashi, Ed.). Sapporo: Hokkaido University Press, p. 129–146.

Hondoh, T. (1992) Glide and climb processes of dislocations in ice. In *Physics and Chemistry of Ice* (N. Maeno and T. Hondoh, Ed.). Sapporo: Hokkaido University Press, p. 481–487.

Hondoh, T. and A. Higashi (1978) X-ray diffraction topographic observations of the large-angle grain boundary in ice under deformation. *Journal of Glaciology*, **21**(85): 629–638.

Hondoh, T. and A. Higashi (1979) Anisotropy of migration and faceting of large-angle grain boundaries in ice bicrystals. *Philosophical Magazine A*, **39**(2): 137–149.

Hondoh, T. and A. Higashi (1983) Generation and absorption of dislocations at large angle grain boundaries in deformed ice crystals. *Journal of Physical Chemistry*, **87**(21): 4044–4050.

Hondoh, T., T. Itoh, S. Amakai, K. Goto and A. Higashi (1983) Formation and annihilation of stacking faults in pure ice. *Journal of Physical Chemistry*, **87**(21): 4040–4044.

Hondoh, T., H. Iwamatsu and S. Mae (1990) Dislocation mobility for non-basal glide in ice measured by *in situ* X-ray topography. *Philosophical Magazine A*, **62**(1): 89–102.

Ignat, M. and H.J. Frost (1987) Grain boundary sliding in ice. *Journal de Physique Colloque C1*, **48**(3): 189–195.

Itagaki, K. (1970) X-ray topographic study of vibrating dislocations in ice under an AC electric field. *Advances in X-ray Analysis*, **13**: 526–538.

Jones, S.J. (1967) Softening of ice crystals by dissolved fluoride ions. *Physics Letters*, **25A**(5): 366–377.

Jones, S.J. and J.W. Glen (1969a) The mechanical properties of single crystals of pure ice. *Journal of Glaciology*, **8**(54): 463–473.

Jones, S.J. and J.W. Glen (1969b) The effect of dissolved impurities on the mechanical properties of ice crystals. *Philosophical Magazine*, **19**(157): 13–24.

Jones, S.J. and N.K. Gilra (1972) Increase of dislocation density in ice by dissolved hydrogen fluoride. *Applied Physics Letters*, **20**(8): 319–320.

Jones, S.J. and N.K. Gilra (1973) X-ray topographical study of dislocations in pure and doped ice. *Philosophical Magazine*, **27**(2): 457–472.

Kamb, W.B. (1961) The glide direction in ice. *Journal of Glaciology*, **3**(30): 1097–1106.

Kobayashi, T. and Y. Furukawa (1975) On twelve branched snow crystals. *Journal of Crystal Growth*, **28**(1): 21–28.

Lang, A.R. (1959) Studies of individual dislocations in crystals by X-ray diffraction micrography *Journal of Applied Physics*, **30**(11): 1748–1755.

Liu, F., I. Baker, M. Yao and M. Dudley (1992) Dislocations and grain boundaries in polycrystalline ice: A preliminary study by synchrotron X-ray topography. *Journal of Materials Science*, **27**(10): 2719–2725.

Liu, F., I. Baker and M. Dudley (1993) Dynamic observations of dislocation generation at grain boundaries in ice. *Philosophical Magazine A*, **67**(5): 1261–1276.

Liu, F., I. Baker and M. Dudley (in press) Thermally induced dislocation loops and stacking faults in polycrystalline ice. *Philosophical Magazine A*.

Mader, H.M. (1992) Observations of the water-vein system in polycrystalline ice. *Journal of Glaciology*, **38**(130): 353–367.

Maeno, N. (1981) *The Science of Ice*. Hokkaido University Press (in Japanese).

Maï, C. (1976) Étude par topographie X du comportement dynamique des dislocations dans la glace Ih. *Comptes Rendus de l'Academie des Sciences de Paris*, **B282**(22): 515–518.

Maï, C., J. Perez, J. Tatibouet and R. Vassoille (1978) Vitesse des dislocations dans la glace dopée avec HF. *Journal de Physique Lettres*, **39**(17): 307–310.

Matsuda, M. and G. Wakahama (1978) Crystallographic structure of polycrystalline ice. *Journal of Glaciology*, **21**(85): 607–620.

Muguruma, J. and A. Higashi (1963) Observations of the etch channels on the (0001) plane of ice crystal produced by non-basal glide. *Journal of the Physical Society of Japan*, **18**(9): 1261–1269.

Murguruma, J., S. Mae and A. Higashi (1966) Void formation by non-basal glide in ice single crystals. *Philisophical Magazine*, **13**(123):625–629.

Mulvaney, R. E.W. Wolff and K. Oates (1988) Sulphuric acid at grain boundaries in Antarctic ice. *Nature*, **331**(6153): 247–249.

Nadgornyi, E. (1988) Dislocation dynamics and mechanical properties of crystals. *Progress in Materials Science*, **31**.

Nakamura, T. and S.J. Jones (1970) Softening effect of dissolved hydrogen chloride in ice crystals. *Scripta Metallurgica*, **4**(2): 123–126.

Nasello, O., C.L. Di Prinzio and L. Levi (1992) Grain boundary migration in bicrystals of ice. In *Physics and Chemistry of Ice* (N. Maeno and T. Hondoh, Ed.). Sapporo: Hokkaido University Press, p. 206–211.

Nye, J.F. (1992) Water veins and lenses in polycrystalline ice. In *Physics and Chemistry of Ice* (N. Maeno and T. Hondoh, Ed.). Sapporo: Hokkaido University Press, p. 200–205.

Oguro, M. (1988) Dislocations in artificially grown single crystals of ice. In *Lattice Defects in Ice Crystals* (A. Higashi, Ed.). Sapporo: Hokkaido University Press, p. 27–47.

Oguro, M. and A. Higashi (1973) Stacking fault images in NH_3-doped ice crystals revealed by X-ray diffraction topography. In *Physics and Chemistry of Ice* (E. Whalley, S.J. Jones and L.W. Gold, Ed.). Ottawa: Royal Society of Canada, p. 338–343.

Oguro, M. and A. Higashi (1981) The formation mechanism of concentric dislocation loops in ice single crystals grown from the melt. *Journal of Crystal Growth*, **51**(1): 71–80.

Oguro, M, and T. Hondoh (1988) Stacking faults in ice crystals. In *Latice Defects in Ice Crystals* (A. Higashi, Ed.). Sapporo: Hokkaido University Press, p. 49–67.

Oguro, M., T. Hondoh and K. Azuma (1988) Interaction between dislocations and point defects in ice crystals. In *Lattice Defects in Ice Crystals* (A. Higashi, Ed.). Sapporo: Hokkaido University Press, p. 97–128.

Ohtomo, M., S. Ahmad and R.W. Whitworth (1987) A technique for the growth of high quality single crystals of ice. *Journal de Physique Colloque C1*, **48**(3): 595–597.

Perez, J., C. Maï and R. Vassoille (1978) Cooperative movement of H_2O molecules and dynamic behaviour of dislocations in ice Ih. *Journal of Glaciology*, **21**(85): 361–374.

Perez, J., C. Maï, J. Tatibouet, and R. Vassoille (1979) Etude des joints de grains dans la glace Ih par meas-ure du frottement intérieur. *Physica status solidi (a)*, **52**(1): 321–330.

Perez, J., C. Maï, J. Tatibouet and R. Vassoille (1980) Dynamic behaviour of dislocations in HF-doped ice I_h. *Journal of Glaciology*, **25**(91): 133–149.

Petrenko, V.F. and E.M. Schulson (1992) The effect of static electric fields on protonic conductivity of ice single crystals. *Philosophical Magazine B*, **66**(3): 341–353.

Petrenko, V.F. and E.M. Schulson (1993) Action of electric fields on the plastic deformation of pure and doped ice single crystals. *Philosophical Magazine A*, **67**(1): 173–185.

Petrenko, V.F. and R.W. Whitworth (1983) Electric currents associated with dislocation motion in ice. *Journal of Physical Chemistry*, **87**(21): 4022–4024.

Petrenko, V.F. and R.W. Whitworth (1994) Structure of ice I_h. Part II: Defects in ice. Volume 1: Point defects. USA Cold Regions Research and Engineering Laboratory, Special Report 94-4.

Rabier, J. and A. George (1987) Dislocations and plasticity in semiconductors II—The relation between dislocation dynamics and plastic deformation. *Revue de Physique Appliquée*, **22**(11): 1327–1351.

Read, W.T. (1953) *Dislocations in Crystals*. New York: McGraw Hill.

Readey, D.W. and W.D. Kingery (1964) Plastic deformation of single crystal ice. *Acta Metallurgica*, **12** (2): 171–178.

Shearwood, C. and R.W. Whitworth (1989) X-ray topographic observations of edge dislocation glide on non-basal planes in ice. *Journal of Glaciology*, **35** (120): 281–283.

Shearwood, C. and R.W. Whitworth (1991) The velocity of dislocations in ice. *Philosophical Magazine A*, **64**(2): 289–302.

Shearwood, C. and R.W. Whitworth (1992) The velocity of dislocations in HCl-doped ice. *Philosophical Magazine A*, **65**(1): 85–89.

Shearwood, C. and R.W. Whitworth (1993) Novel processes of dislocation multiplication observed in ice. *Acta Metallurgica et Materialia*, **41**(1): 205–210.

Sinha, N.K. (1977) Dislocations in ice as revealed by etching. *Philosophical Magazine*, **36**(6): 1385–1404.

Sutton, A.P. (1984) Grain boundary structure. *International Metals Reviews*, **29**(5): 377–402.

Suzuki, S. and D. Kuroiwa (1972) Grain boundary energy and grain boundary groove angles in ice. *Journal of Glaciology*, **11**(62): 265–277.

Tatibouet, J., J. Perez and R. Vassoille (1986) High temperature internal friction and dislocations in ice Ih. *Journal de Physique*, **47**(1): 51–60.

Tatibouet, J., J. Perez and R. Vassoille (1987) Study of grain boundaries in ice by internal friction measurement. *Journal de Physique Colloque C1*, **48**(3): 197–203.

Unwin, P.N.T. and J. Muguruma (1972) Electron microscope observations on the defect structure of ice. *Physica Status Solidi (a)*, **14**(1): 207–216.

Vassoille, R., C. Maï and J. Perez (1978) Inelastic behaviour of ice Ih single crystals in the low-frequency range due to dislocations. *Journal of Glaciology*, **21**(85): 375–384.

Webb, W.W. and C.E. Hayes (1967) Dislocations and

plastic deformation of ice. *Philosophical Magazine*, **16**(143): 909–925.

Weertman, J. (1963) The Eshelby-Shoeck viscous dislocation damping mechanism applied to the steady-state creep of ice. In *Ice and Snow: Properties, Processes and Applications* (W.D. Kingery, Ed.). Cambridge Massachusetts: MIT Press, p. 28–33.

Weertman, J. (1973) Creep of ice. In *Physics and Chemistry of Ice* (E. Whalley, S.J. Jones and L.W. Gold, Ed.). Ottawa: Royal Society of Canada, p. 320–397.

Whitworth, R.W. (1975) Charged dislocations in ionic crystals. *Advances in Physics*, **24**(2): 203–304.

Whitworth, R.W. (1980) The influence of the choice of glide plane on the theory of the velocity of dislocations in ice. *Philosophical Magazine A*, **41**(4): 521–528.

Whitworth, R.W. (1983) Velocity of dislocations in ice on {0001} and {$10\bar{1}0$} planes. *Journal of Physical Chemistry*, **87**(21): 4074–4078.

Whitworth, R.W., J.G. Paren and J.W. Glen (1976) The velocity of dislocations in ice—A theory based on proton disorder. *Philosophical Magazine*, **33**(3): 409–426.

Wolff, E.W. and J.G. Paren (1984) A two phase model of electrical conduction in polar ice sheets. *Journal of Geophysical Research*, **89**(B11): 9435–9438.

Wolff, E.W., R. Mulvaney and K. Oates (1988) The location of impurities in Antarctic ice. *Annals of Glaciology*, **11**: 194–197.

REPORT DOCUMENTATION PAGE

Form Approved
OMB No. 0704-0188

1. AGENCY USE ONLY (Leave blank)	2. REPORT DATE	3. REPORT TYPE AND DATES COVERED
	May 1994	

4. TITLE AND SUBTITLE
Structure of Ordinary Ice I_h
Part II: Defects in Ice
Volume 2: Dislocations and Plane Defects

5. FUNDING NUMBERS

6. AUTHORS
Victor F. Petrenko and Robert W. Whitworth

7. PERFORMING ORGANIZATION NAME(S) AND ADDRESS(ES)
U.S. Army Cold Regions Research and Engineering Laboratory, Hanover, New Hampshire
Thayer School of Engineering, Dartmouth College, Hanover, New Hampshire
University of Birmingham, Birmingham, United Kingdom

8. PERFORMING ORGANIZATION REPORT NUMBER
Special Report 94-12

9. SPONSORING/MONITORING AGENCY NAME(S) AND ADDRESS(ES)
Army Research Office
Research Triangle Park
Durham, North Carolina 27709

10. SPONSORING/MONITORING AGENCY REPORT NUMBER

11. SUPPLEMENTARY NOTES

12a. DISTRIBUTION/AVAILABILITY STATEMENT
Approved for public release; distribution is unlimited.
Available from NTIS, Springfield, Virginia 22161.

12b. DISTRIBUTION CODE

13. ABSTRACT (*Maximum 200 words*)

This report examines linear and planar defects in ice: dislocations, grain boundaries and stacking faults. The authors review experimental results and theoretical models on the defects' atomic structures and physical properties. In addition, experimental techniques used for direct observation of defects, experimental results and theoretical interpretation of dislocation mobility and the role of dislocations in plastic deformation are considered.

14. SUBJECT TERMS
Ice
Ice molecular structure
Ice physics
Linear defects
Planar defects

15. NUMBER OF PAGES
32

16. PRICE CODE

17. SECURITY CLASSIFICATION OF REPORT	18. SECURITY CLASSIFICATION OF THIS PAGE	19. SECURITY CLASSIFICATION OF ABSTRACT	20. LIMITATION OF ABSTRACT
UNCLASSIFIED	UNCLASSIFIED	UNCLASSIFIED	UL